Molecular characteristics of diel rhythmic diversity reveal disconnection between different levels of organismal rhythmicity

AUTHORS

N. Sören Häfker[1,2,*], Laurenz Holcik[1,3,4], Karim Vadiwala[1,2,‡], Isabel Beets[5], Alexander W. Stockinger[1,2,3], Stefan Hammer[1,§], Liliane Schoofs[5], Florian Raible[1,2], Kristin Tessmar-Raible[1,2,*]

AFFILIATIONS

[1] Max Perutz Labs, University of Vienna, Vienna BioCenter, Dr. Bohr-Gasse 9/4, 1030 Vienna, Austria

[2] Research Platform "Rhythms of Life", University of Vienna, Vienna BioCenter, Dr. Bohr-Gasse 9/4, 1030 Vienna, Austria

[3] Vienna BioCenter PhD Program, Doctoral School of the University of Vienna, Medical University of Vienna, 1030 Vienna, Austria

[4] Center for Integrative Bioinformatics Vienna, Max Perutz Labs, University of Vienna, Medical University of Vienna, Dr. Bohr-Gasse 9/4, 1030 Vienna, Austria

[5] Division of animal Physiology and Neurobiology, KU Leuven, Naamsestraat 59, 3000 Leuven, Belgium

[‡] current address: EUCODIS Bioscience GmbH, Campus Vienna Biocenter 2, 1030 Vienna, Austria

[§] current address: Institut für Diskrete Mathematik, TU Graz, Steyrergasse 30/III, A-8010 Graz, Austria

* Correspondence: kristin.tessmar@mfpl.ac.at (K.T.-R.), soeren_haefker@web.de (N.S.H.)

HIGHLIGHTS

- Individual worms show diverse yet persistent diel behavioral rhythms.
- Behavioral rhythm diversity does not match clock gene expression and *pdf* function.
- Behaviorally arrhythmic worms exhibit strong diel cycling of metabolic transcripts.
- Behaviorally rhythmic worms exhibit strong diel cycling of neuronal transcripts.

ABSTRACT

The 24 hour day/night cycle prominently controls behavior and physiology. Most diel behaviors are under circadian clock control, but behavioral rhythmicity also exhibits significant individual diversity. Even genetically identical clones raised under the same conditions can develop distinct behavioral mannerisms[1,2]. While terrestrial model systems have provided key molecular insights, the variability and molecular basis of diel rhythms in marine animals are much less investigated, although critically informative for evolutionary and ecological hypotheses.

Here we investigate the phenotypic diversity of diel locomotor rhythms in the marine annelid *Platynereis dumerilii*. Individual-specific diel activity patterns are maintained over time, but differ strongly even between co-raised siblings. Knock-out of pigment-dispersing factor (PDF), a neuropeptide central to diel rhythmicity in *Drosophila melanogaster*[3], reveals only limited contributions of PDF to rhythmic behavioral diversity. Diel transcriptomes sampled from behaviorally rhythmic versus arrhythmic worms show no differences in circadian core clock transcript oscillations. Instead, behaviorally rhythmic worms exhibit a distinct enrichment of cycling transcripts related to behavior and neuronal differentiation, while behaviorally arrhythmic worms show an enrichment of metabolic and transport-related diel-cycling transcripts. Cycling of matrix metalloproteinases suggests that individual rhythmicity may be influenced via extracellular matrix remodeling and neuropeptide processing[4].

Our results emphasize that organismal rhythmicity is highly complex and not necessarily properly reflected by a single read-out (like behavior or clock gene expression). We hypothesize that diversity in diel behavioral patterns allows for an adjustment to (micro)habitat conditions in the wild, thereby impacting on population fitness and adaptability to changing environmental conditions.

KEY WORDS

individuality, *Platynereis*, behavior, metabolism, diel rhythmicity, circadian, clock, pigment-dispersing factor, chronotype, transcriptome, matrix metalloproteinase, adaptation

INTRODUCTION

Life on earth has been evolving in the presence of numerous environmental cycles. This is particularly prominent in the marine environment[5,6], where rhythms even exist in the deep sea[7]. In the oceans, biological rhythms can be the major factors shaping ecosystem structure and productivity, and they significantly contribute to biogeochemical cycling[8–10], but compared to the terrestrial environment our understanding of the factors and mechanisms driving marine rhythmicity is still severely limited[6]. This is particularly concerning in the context of climate change as it is largely unknown how marine timing systems and associated species fitness on the individual and population level will be affected by changing environmental conditions[6,11].

Rhythmic adaptations on the level of behavior, physiology and gene expression are central in shaping an animal's interaction with the abiotic and biotic environment. Many of these rhythms are under the control of endogenous timing mechanisms (clocks)[11,12]. By far best studied is the circadian clock that enables organisms to synchronize (entrain) to, and to anticipate the 24 hour day/night cycle[13], thereby significantly contributing to fitness[14,15].

77 Animal behavior can be highly diverse among individuals, even if they are closely
78 related or were raised under the same conditions. This behavioral individuality – also referred
79 to as 'personality', 'behavioral syndrome' or 'coping style' – is consistent over time and has
80 been described in a variety of organisms from invertebrates to mammals[16–18]. Individual
81 phenotypes can be explained by genetic predisposition[19–21], epigenetic effects [22,23], or
82 conditions experienced in the (micro)environment[1,24]. However, a broader understanding of
83 gene expression dynamics and metabolic pathways differing between phenotypically distinct
84 individuals is in general still limited and even non-existent for marine species [21,25–27].

85 Behavioral diversity can be displayed in many forms including differences in overall
86 activity, responses to stimuli, and social interactions[17,28] and is also highly prominent in diel
87 rhythms of behavior [29,30]. Studies in terrestrial organisms, like drosophilid flies, identified
88 differences in the expression of circadian clock genes and the neuropeptide pigment-
89 dispersing factor (PDF) to be responsible for species- and population-specific patterns of diel
90 activity[3,20,21,31–33]. Similarly, differences in clock gene expression rhythms were linked to
91 caste-specific activity phenotypes in ants[26]. Comparisons of fly strains and species from
92 different latitudes further indicate that behavioral rhythmicity depends on the localization of
93 circadian core clock genes expression in the brain [32,34] and clock gene alleles [35,36].
94 Furthermore, behavioral phenotypes including arrhythmicity can also depend on the circadian
95 clock output pathways[33]. However, there are no studies that address individual rhythmic
96 diversity and its possible interplay with endogenous timers in marine animals.

97 The marine polychaete *Platynereis dumerilii* is a molecularly slowly evolving annelid
98 that has emerged as a functional model for marine chronobiology with a life cycle
99 representative for various marine invertebrates[37–40]. After a planktonic phase during which
100 larvae get dispersed by currents, the worm switches to a benthic lifestyle[37]. For marine
101 broadcast spawners like *P. dumerilii*, the possibilities to select the habitat they encounter upon

settling can be very limited. The worms inhabit temperate to tropical shores worldwide, typically at depths of 0-10 m[41,42].

Here, we explore diel behavioral diversity of *P. dumerilii* strains and individuals, its transcriptome-wide consequences and the role of PDF, an important neuropeptide for behavioral rhythmicity in *Drosophila melanogaster*[3,31]. Worms display strain-specific characteristics as well as strong and reproducible inter-individual variability in diel behavior, even among co-raised siblings. Worms carrying knock-out mutations for the *pdf* gene can exhibit behavioral rhythmicity reduction, but the phenotype is strongly strain-dependent. This suggests additional internal factors as prominent regulators of diel behavioral patterns. Indeed, diel transcriptome comparisons of behaviorally rhythmic versus arrhythmic worms show no differences in the expression of circadian clock genes or *pdf*. The data reveal clear differences in the oscillation amplitudes of diel cyclic transcripts, especially for transcripts involved in neuronal signaling versus metabolic processes. Our findings further point towards a potential role of neuronal differentiation/remodeling processes in the establishment of rhythmic individual phenotypes. Considering the complexity of the cyclic environment in marine habitats[5,6], unraveling the molecular processes shaping phenotypic rhythms and their diversity will be important to understand how marine species adapt to these conditions, and how individuals and populations cope the ongoing shifts in habitat conditions due to climate change.

RESULTS

P. dumerilii diel behavioral rhythmicity differs between strains and especially individuals

In our previous studies, we repeatedly noticed a high diversity in the diel/circadian behavior of immature and premature *Platynereis dumerilii* bristle worms[39,43,44]. This prompted us to systematically investigate the worms' diversity in diel locomotor rhythmicity patterns. Below

we use the term 'rhythmicity/arrhythmicity' to specifically refer to behavior, while we use the term 'cycling' in the context of gene expression.

We chose 3 worm strains (VIO & PIN: collected from the Bay of Naples, Italy more than 50 years ago and continuously incrossed over the past 14 years; NAP: newly collected from the Bay of Naples in 2009 and maintained as a non-incrossed, closed culture)[40,45]. We repeatedly recorded locomotor behavior of immature/premature sibling worms for 4 days of 16h:8h light/dark-cycle (LD) followed by 4 days of constant darkness (DD) (Fig.1A). All strains were generally nocturnal and showed little inter-strain differences in morning/afternoon/night activity (Fig.1B). However, when we analyzed diel rhythmicity (20h-28h period range) under LD and DD in more detail, we saw strain-specific rhythmicity patterns and rhythm power varied significantly between strains (Fig.1A,C-G, Fig.S2). Aside the inter-strain differences, all strains displayed pronounced inter-individual variability in rhythm power that is best described as a behavioral continuum reaching from highly rhythmic to fully arrhythmic worms (Fig.1C,D and Fig.D1 in the Dryad dataset of this paper).

To closer investigate the observed individual diversity, we performed repetition runs on a total of 30 worms (PIN n= 12, NAP n=5, VIO n=13) 1-2 months after the initial recordings. Actograms of the first and second recordings were very reproducible for most individual worms showing the same behavioral characteristics in both runs (Fig.1E-G, Fig.S2). Of note, after the initial run we kept all worms individually for identification, which are different conditions from the "group maintenance" that the worms experienced before the initial run. The highest diversity of behavioral patterns was observed in PIN worms, which, however, also exhibited the highest consistency between initial and repeated runs. Compared to the differences between strains (Fig.1A-D), inter-individual diversity in behavioral rhythms is much larger. This shows that diel activity patterns in *P. dumerilii* are not only highly variable between siblings, but are also highly reproducible in individuals over time.

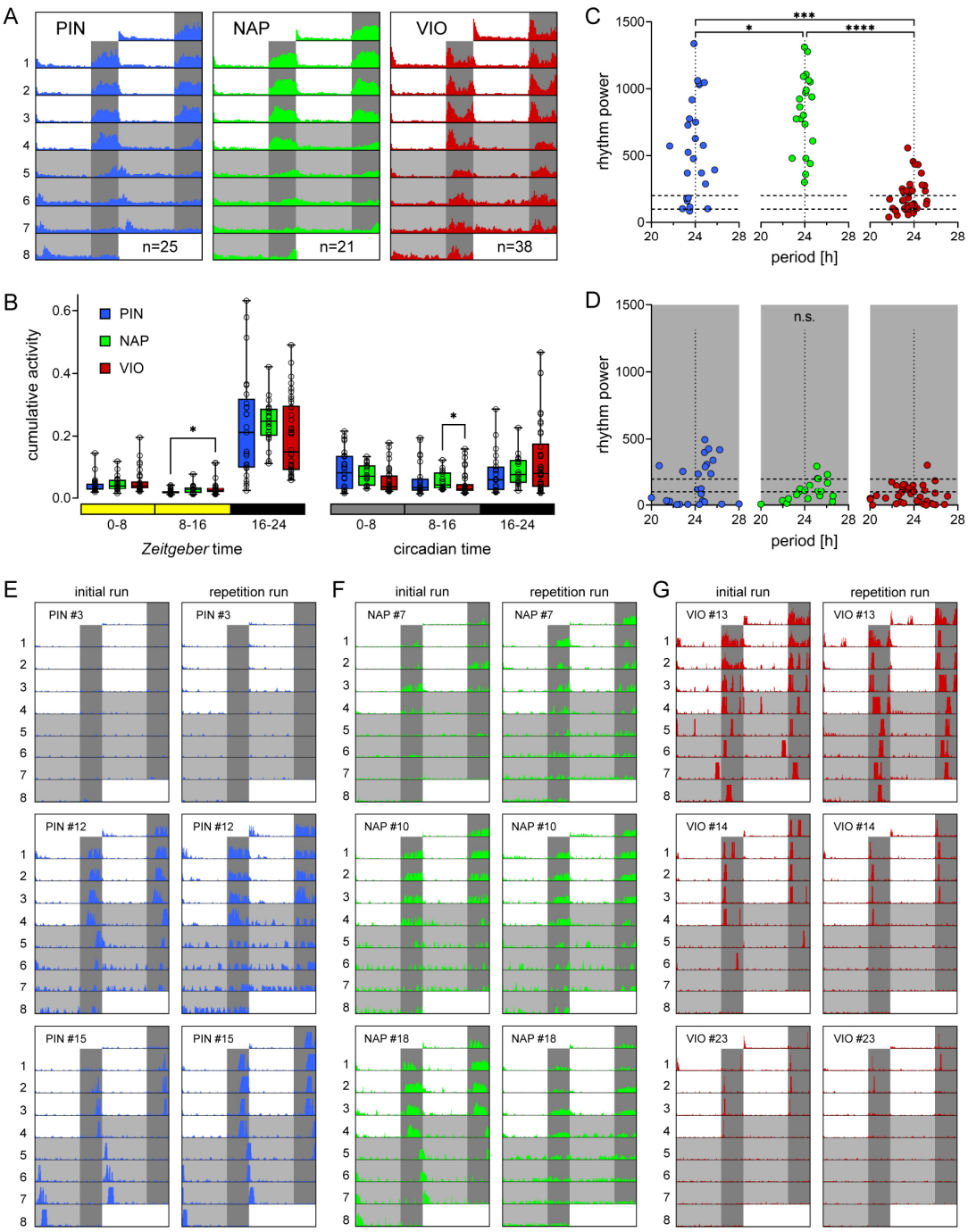

Figure 1: Inter-strain and inter-individual variability in diel behavioral rhythmicity. The diel locomotor activities of the three *P. dumerilii* strains PIN (n=25, blue), NAP (n=20, green) and VIO (n=37, red) are compared. (A) Double-plotted actograms showing mean locomotor activity over 4 days of a 16h:8h light/dark-cycle (LD) followed by 4 days of constant darkness (DD). Individual worm actograms were submitted to Dryad (Fig.D1). (B) Cumulative activity over the early day (0-8), late day (8-16) and night (16-24) in LD and DD (shaded background). Box indicates median and 25%/75% percentiles, whiskers indicate min/max values. Each circle represents an individual worm. (C,D) Period/power of locomotor rhythms in the diel/circadian range (20h-28h) in LD and DD (shaded background) determined by Lomb-Scargle periodogram. Each circle represents an individual worm. Dashed horizontal lines indicate thresholds for weak rhythm power (<200) and arrhythmicity (<100) based on visual actogram inspection. (E-G) Actograms of PIN, NAP and VIO individual worms investigated in two consecutive runs (initial/repeated). Per strain, three individuals are shown. # indicates the individual worm number. In total,

12 PIN worms, 5 NAP worms and 13 VIO worms were investigated twice. Statistical differences were determined via Kruskal-Wallis ANOVA on Ranks (panels B,D) or Welch's ANOVA (panel C). Significance levels: *p<0.05, **p<0.01, ***p<0.001, ****p<0.0001. Actograms of repeated individuals not shown here are provided in Fig.S1.

Characterization of pigment-dispersing factor

To gain deeper insight into potential molecular causes of the observed individual rhythmic diversity, we investigated pigment-dispersing factor (PDF), a conserved neuropeptide that is central to the communication and output of circadian clock neurons, thereby shaping diel rhythmicity in drosophilid flies and other insects[3,46]. *P. dumerilii* sequences of the PDF precursor protein (prepro-PDF) and PDF-receptor (PDFR) were identified (see methods) and compared to similar sequences from other species in phylogenetic analyses (Fig.2A,B, Tab.S1). This confirmed the identity of our PDF and PDFR sequences and the separation of PDFR from the closely related calcitonin-/diuretic hormone 31-receptors [47].

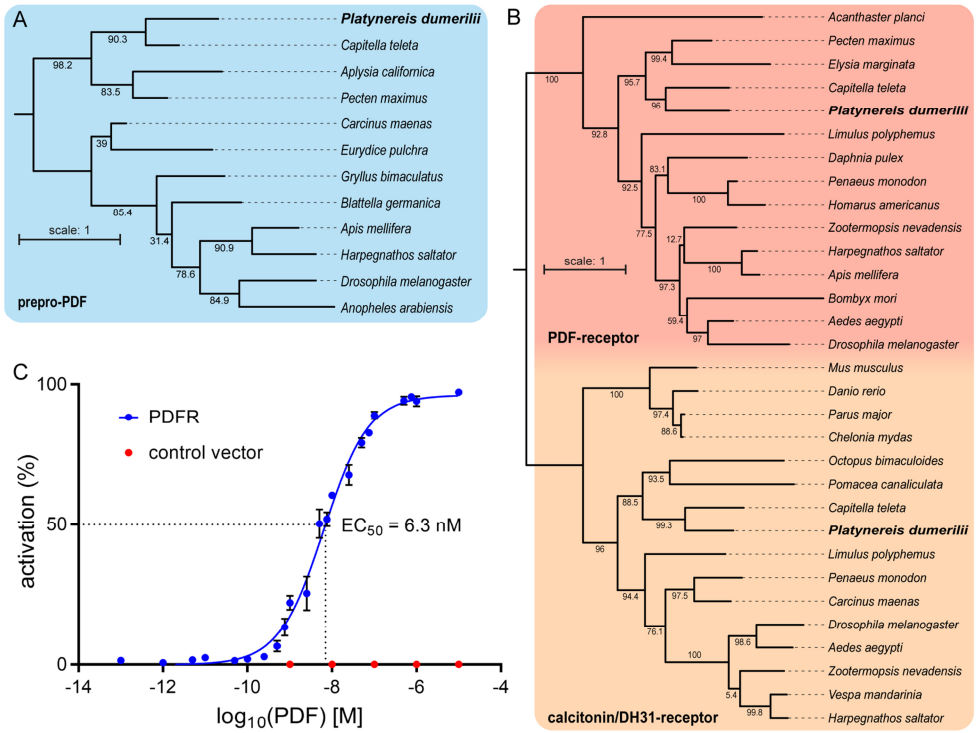

Figure 2: PDF and PDF-receptor phylogeny and deorphanization. Maximum-likelihood phylogenetic trees of (A) the pigment-dispersing factor precursor protein (prepro-PDF) and (B) the pigment-dispersing factor receptor (PDF-receptor) as well as calcitonin-receptor and diuretic hormone 31 (DH31) receptor. See supplement for peptide sequences used for tree construction (Tab.S1). (C) Activation curve of the *P.dumerilii* PDF-receptor by PDF (blue) with EC_{50} indicating the concentration needed for 50% receptor

activation (n=10-12 per concentration). Red dots indicate activation after transfection with empty control vector (n=6 per concentration). Mean values ± SEM are shown (Tab.S2).

To validate the functionality of the PDF/PDFR-system in *P. dumerilii, pdfr* was expressed in CHO cells employing an *apoaequorin/human Gα16 subunit* reporter system[48]. The assay confirmed that in *P. dumerilii* PDFR can be activated by PDF at physiological concentrations (EC_{50}=6.3 nM, Fig.2C).

Next, we induced mutations in the *pdf* gene of VIO wildtype worms using TALENs[49], resulting in insertion/deletions in the 3rd exon preceding the start of the mature peptide sequence (Fig.3A,B). We checked F_1-outcrossed worms for changes in the *pdf* sequence. Worms that showed frame-shift mutations and early stop codons were again crossed against VIO wildtypes, and the resulting heterozygous offspring were incrossed. Thereby we established two mutant lines with a -14bp deletion and a +4bp insertion, respectively (Fig.3A,B). Both alleles are predicted to result in a complete failure of mature peptide generation (Fig.3B).

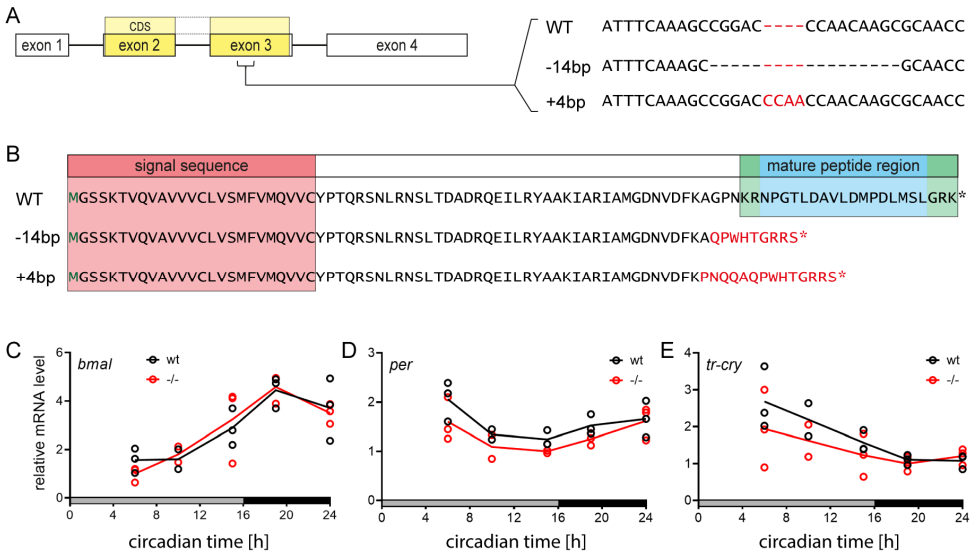

Figure 3: TALENs-induced *pdf* gene knockout and effects on clock genes. (A) TALENs (transcription activator-like effector nucleases) targeting exon 3 of the *pdf* gene were used to induce frame shift mutations in the coding sequence (CDS). Two mutant strain with a -14bp deletion and a +4bp insertion were established, respectively. (B) Translated peptide sequence of the *pdf* gene. Start codon methionine (green M), signal sequence for cellular export (red background), cleavage regions (green background) and mature peptide (blue background) are indicated. Both frame shift mutations led to a premature stop codon (*) and a complete loos of the mature PDF peptide. (C) Circadian expression of the clock genes *bmal*, *per*, and *tr-cry* in *pdf* wildtypes and mutants. Samples were collected on the 2nd day of DD after previous LD (16h:8h) entrainment. Per time point, n=3 replicates were measured (n=2 for circadian time 10). Student's t-tests for

209 each time points found no significant differences between wildtypes and mutants. Raw C_t-values are
210 provided in the supplement (Tab.S3).
211 To determine potential effects of *pdf* loss on the circadian clock, we compared the expression
212 of the clock genes *bmal*, *per* and *tr-cry* in *pdf* wildtypes and -14/-14 mutants (VIO
213 background). Worms were entrained to a LD cycle (16h:8h) and expression in the head was
214 analyzed by qPCR on the 2nd day of DD at 5 circadian time points. Unpaired 2-side t-tests
215 found no significant differences between wildtypes and mutants for any gene and time point
216 (Fig.3C-E).
217
218 *pdf* mutants show strain-dependent reduction in diel behavioral rhythmicity
219 To investigate the role of PDF in *P. dumerilii* diel locomotor rhythms, the activity of *pdf*
220 wildtypes and mutants in the VIO strain background were recorded in LD (16h:8h) and DD
221 (Fig.4A). *pdf* mutants showed significantly lower rhythm power in both LD and DD. In
222 contrast, the same mutation in the PIN strain background did not show this phenotype
223 (Fig.4B). Under LD, PIN-crossed wildtypes were in fact slightly less rhythmic than mutants.
224 The behavioral characterizations showed no within-strain differences between mutant alleles
225 (-14/-14, +4/+4), as well as transheterozygous worms (-14/+4), and thus data were combined
226 (Fig.D2 in Dryad). The results suggest that PDF is not a major determinant of diel behavioral
227 rhythmicity in *P. dumerilii*, indicative of additional important molecular players with major
228 effects on worm rhythmicity and individual phenotypes.
229
230 Transcriptomics reveal cycling clock genes in both rhythmic and arrhythmic worm
231 phenotypes
232 To gain a broader understanding of the molecular characteristics associated with diel
233 behavioral rhythmicity, we investigated the diel transcriptome of rhythmic and arrhythmic
234 wildtype worms. We focused on worms of the PIN strain, as their diel activity patterns

showed the most pronounced inter-individual diversity, but also the strongest within-individual consistency (Fig.1, FigS2).

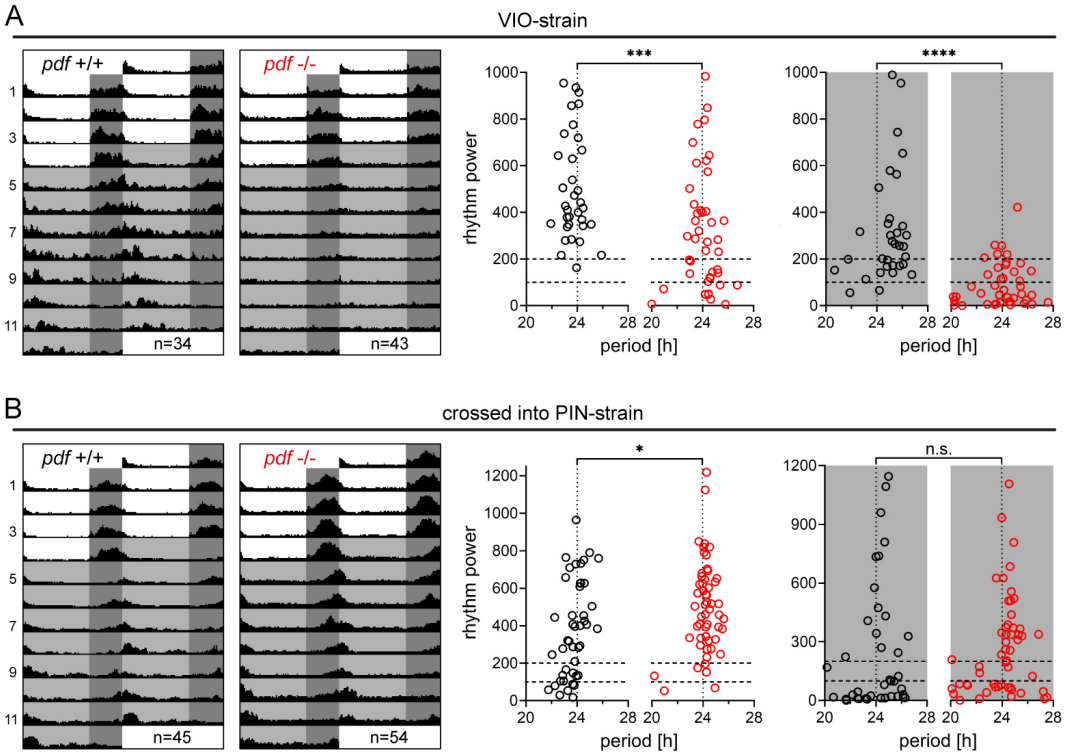

Figure 4: Role of *pdf* in diel behavioral rhythmicity. (A) Diel/circadian locomotor activity of VIO-strain *pdf* wildtypes (n=34, black) and mutants (n=43, red) under 4 days of LD and 5 or 8 days of DD. (B) Diel/circadian locomotor activity of PIN-strain crossed wildtypes (n=45, black) and mutants (n=54, red) under 4 days of LD and 4 or 8 days of DD. For each strain, double-plotted mean actograms as well as period/power of locomotor rhythms in the diel/circadian range (20h-28h) in LD and DD (shaded background) are shown. Dashed horizontal lines indicate thresholds for weak rhythm power (<200) and arrhythmicity (<100) based on visual actogram inspection. Statistical differences were determined via Mann-Whitney U-test. Significance levels: *p<0.05, **p<0.01, ***p<0.001, ****p<0.0001. Individual worm actograms were submitted to Dryad (Fig.D2).

Behavior of wildtype worms was recorded for 3 LD days and 3 DD days, and worms were characterized as either rhythmic (clear 24h rhythmicity), arrhythmic (no rhythmicity) or unclear (everything in between) based on visual actogram inspection and ActogramJ rhythm analysis (Fig.5A and Fig.D3 in Dryad). As already observed for the strain comparison, there was a behavioral continuum with many worms showing intermediate phenotypes. Head samples of clearly rhythmic and clearly arrhythmic worms were then collected under LD in 4h intervals starting at ZT0 (lights on), and with 3 replicates per time point. Due to the work-intensive phenotypic characterization, samples had to be collected discontinuously and not 'in

one go'. Transcriptomics were performed on a NextSeq550 System (Illumina, USA) and resulted in a total of 445,553,522 raw reads (Fig.5B). Trimming/filtering caused a 0.48% read loss and trimmed reads were mapped against an independently generated transcriptome (see methods). The mapping results were filtered to exclude transcripts that were not/hardly expressed and/or were <500bp, resulting in 48,605 distinct expressed transcripts (Tab.S4).

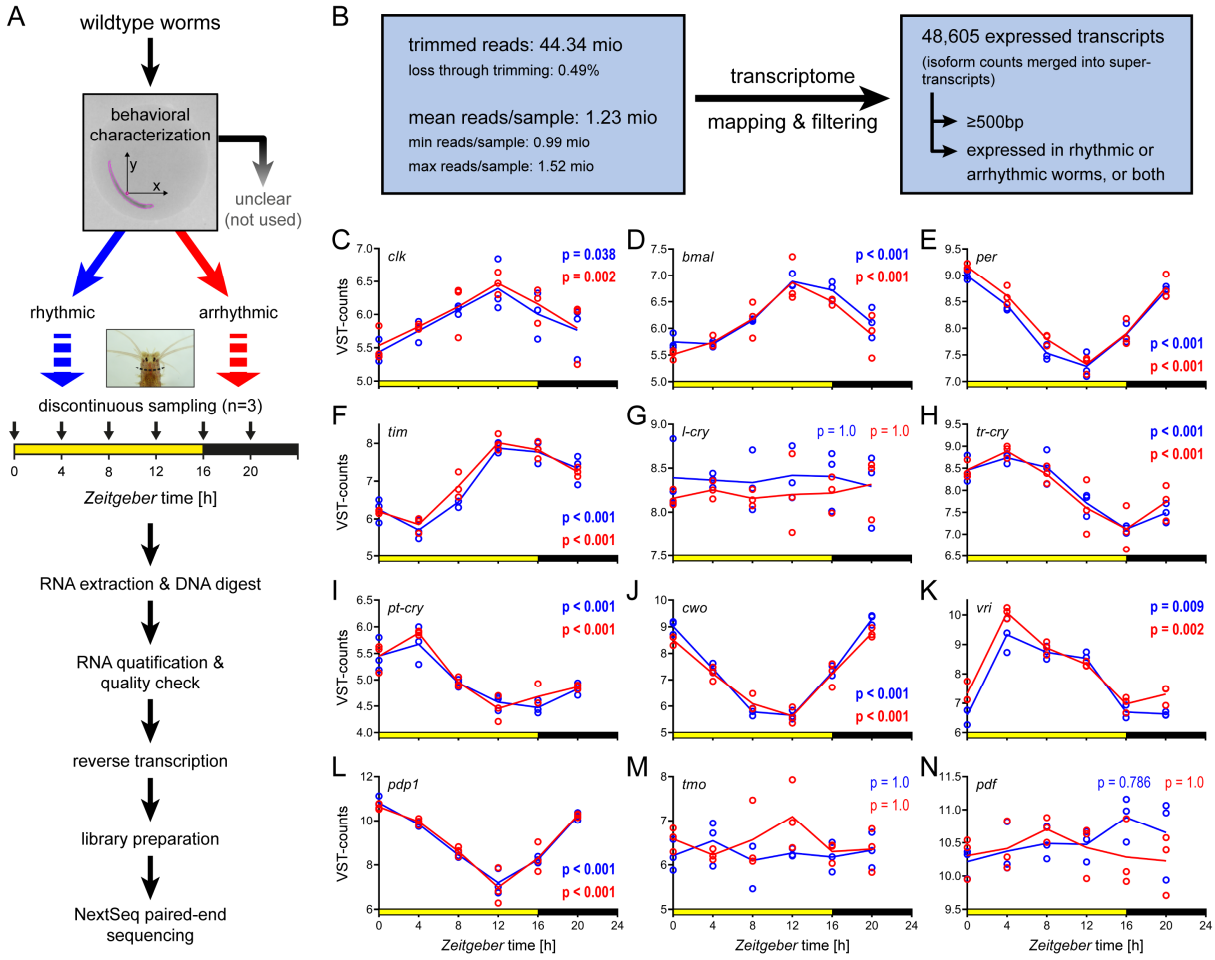

Figure 5: Transcriptome generation from rhythmic/arrhythmic *P. dumerilii* wildtype worms. (A) Diel locomotor behavior of PIN-strain wildtypes was characterized as rhythmic (blue) or arrhythmic (red). Individual actograms including characterizations were submitted to Dryad. Worm heads were sampled discontinuously over a 16h:8h LD cycle (n=3 per time point, 3 heads pooled per replicate) and samples were processed for NextSeq transcriptome sequencing. (B) Overview of the reads and expressed transcripts produced by the sequencing. (C-N) Diel expression patterns of circadian clock genes and *pdf*. p-values show results of RAIN rhythm analysis with bolt values indicating significant 24h cycling. Per time point, n=3 replicates were measured. For abbreviations of clock genes and detailed RAIN results see Tab.S4.

We first focused on core circadian clock genes (Fig.5C-N) and overall transcriptome rhythmicity. Core circadian clock genes of the behaviorally rhythmic worms also served as

273 benchmark to assess if the discontinuous sampling (see above) affected transcriptome
274 rhythmicity. Reassuringly, core circadian clock gene cycling closely mirrored previous
275 reports[39,43,50]. Of note, neither the core circadian clock transcripts, nor the *pdf* transcript
276 showed significant differences in cyclic expression between rhythmic and arrhythmic worms
277 (Fig.5C-N).

278 To further look for possible differences in transcriptomic cycling between rhythmic and
279 arrhythmic worms, we identified transcripts with 24h cyclic expression via RAIN[51]. The
280 analysis detected a total of 1451 transcripts (2.99% of all expressed transcripts) with 24h
281 cycling in rhythmic worms (n=603), arrhythmic worms (n=554), or both phenotypes (n=294)
282 (Fig.6A, Tab.S4). For the core circadian clock genes, RAIN found significant cycling in all of
283 them for both phenotypes, except for *l-cry*, *tmo* and *pdf* (Fig.5C-N), consistent with previous
284 results[43,50,52]. Aside from the core circadian clock transcripts, both phenotypes showed
285 significant cycling of transcripts for *6-4 photolyase*, *r-opsin3*, G_o*-opsin1* and *myocyte*
286 *enhancer factor 2* (*mef2*) (Tab.S4). Furthermore, several transcripts encoding matrix
287 metalloproteinases (MMPs) were found to cycle in rhythmic worms (n=3), arrhythmic worms
288 (n=2), or both phenotypes (n=3) (Fig.S3, Tab.S6).

289

290 <u>Gene ontology analyses point at strong metabolic rhythmicity in behaviorally arrhythmic</u>
291 <u>worms</u>

292 To identify cyclic biological functions and processes associated with rhythmic or arrhythmic
293 worms, we performed a systematic gene ontology (GO) analyses. RAIN-significant
294 transcripts cycling in rhythmic, arrhythmic or both phenotypes were compared against all
295 expressed 48,605 unique transcript IDs to determine overrepresented GO-terms for each
296 group (Fig.6, Tab.S5). Compared to all expressed transcripts, 77 GO-terms were enriched in
297 the transcript cycling in rhythmic worms, 29 in the transcripts cycling in arrhythmic worms,
298 and 25 terms in the transcripts cycling in both phenotypes (Tab.S5).

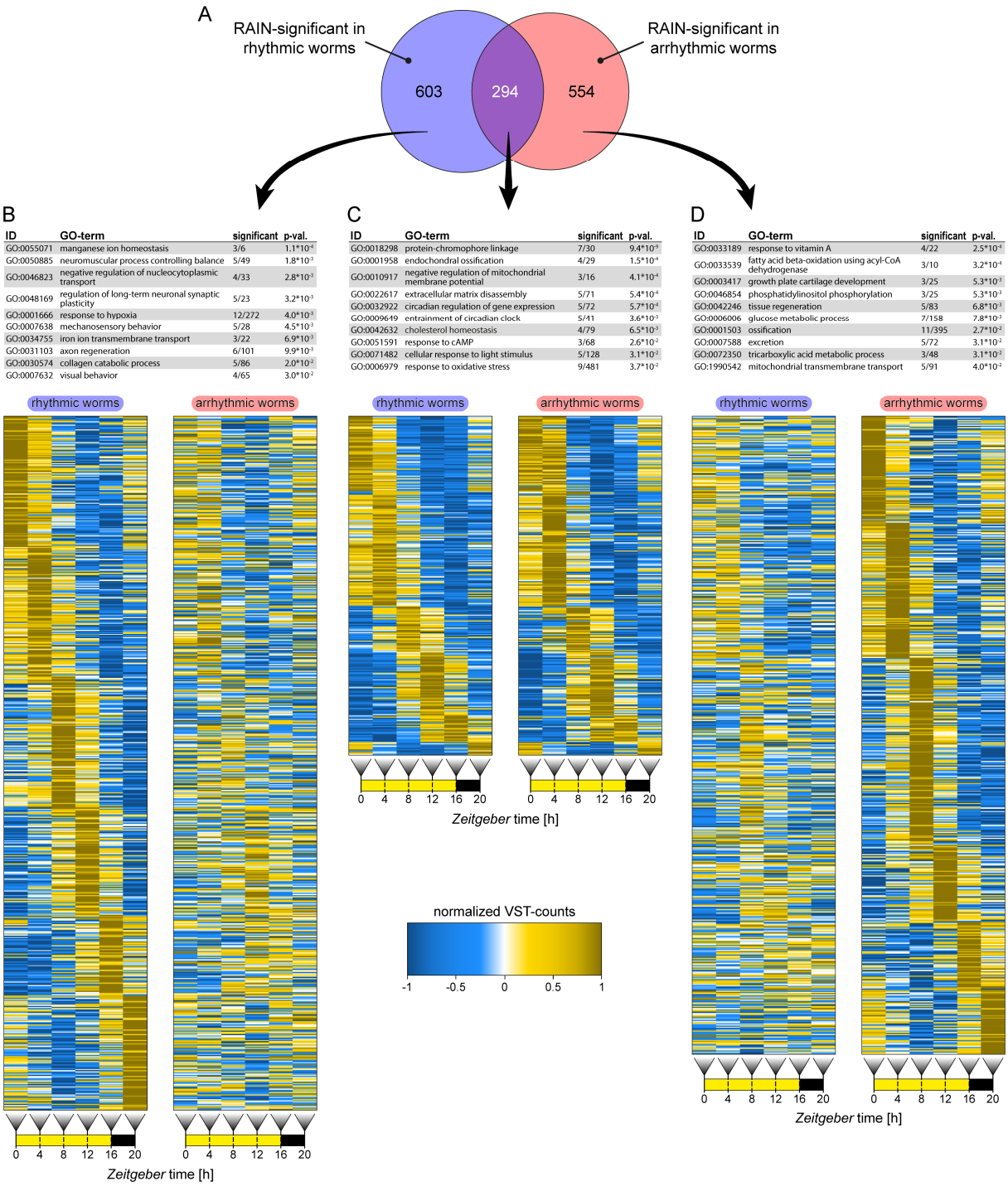

B

ID	GO-term	significant	p-val.
GO:0055071	manganese ion homeostasis	3/6	$1.1*10^{-4}$
GO:0050885	neuromuscular process controlling balance	5/49	$1.8*10^{-3}$
GO:0046823	negative regulation of nucleocytoplasmic transport	4/33	$2.8*10^{-3}$
GO:0048169	regulation of long-term neuronal synaptic plasticity	5/23	$3.2*10^{-3}$
GO:0001666	response to hypoxia	12/272	$4.0*10^{-3}$
GO:0007638	mechanosensory behavior	5/28	$4.5*10^{-3}$
GO:0034755	iron ion transmembrane transport	3/22	$6.9*10^{-3}$
GO:0031103	axon regeneration	6/101	$9.9*10^{-3}$
GO:0030574	collagen catabolic process	5/86	$2.0*10^{-2}$
GO:0007632	visual behavior	4/65	$3.0*10^{-2}$

C

ID	GO-term	significant	p-val.
GO:0018298	protein-chromophore linkage	7/30	$9.4*10^{-3}$
GO:0001958	endochondral ossification	4/29	$1.5*10^{-4}$
GO:0010917	negative regulation of mitochondrial membrane potential	3/16	$4.1*10^{-4}$
GO:0022617	extracellular matrix disassembly	5/71	$5.4*10^{-4}$
GO:0032922	circadian regulation of gene expression	5/72	$5.7*10^{-4}$
GO:0009649	entrainment of circadian clock	5/41	$3.6*10^{-3}$
GO:0042632	cholesterol homeostasis	4/79	$6.5*10^{-3}$
GO:0051591	response to cAMP	3/68	$2.6*10^{-2}$
GO:0071482	cellular response to light stimulus	5/128	$3.1*10^{-2}$
GO:0006979	response to oxidative stress	9/481	$3.7*10^{-2}$

D

ID	GO-term	significant	p-val.
GO:0033189	response to vitamin A	4/22	$2.5*10^{-4}$
GO:0033539	fatty acid beta-oxidation using acyl-CoA dehydrogenase	3/10	$3.2*10^{-4}$
GO:0003417	growth plate cartilage development	3/25	$5.3*10^{-3}$
GO:0046854	phosphatidylinositol phosphorylation	3/25	$5.3*10^{-3}$
GO:0042246	tissue regeneration	5/83	$6.8*10^{-3}$
GO:0006006	glucose metabolic process	7/158	$7.8*10^{-3}$
GO:0001503	ossification	11/395	$2.7*10^{-2}$
GO:0007588	excretion	5/72	$3.1*10^{-2}$
GO:0072350	tricarboxylic acid metabolic process	3/48	$3.1*10^{-2}$
GO:1990542	mitochondrial transmembrane transport	5/91	$4.0*10^{-2}$

Figure 6: Transcriptome RAIN analysis and gene ontologies. (A) RAIN analysis identified 1643 transcript with significant 24 hour cycling in rhythmic worms (blue), arrhythmic worms (red), or both. (Tab.S4). (B-D) The top 10 GO-terms for each group are shown, and full lists of significant terms are provided in the supplement (Tab.S5). Diel expression of RAIN-significant transcripts for each group are plotted as heatmaps for rhythmic and arrhythmic worms. Heatmaps are based on mean VST-counts and are sorted by diel peak expression times. Expression is normalized for both phenotypes together, meaning amplitudes are comparable between rhythmic and arrhythmic worms, but not between different transcripts. For detailed RAIN results see Tab.S4.

309 Cycling transcripts shared by worms of both phenotypes showed enrichment in GO-terms
310 associated in rhythmic/circadian processes such as 'circadian regulation of gene expression'
311 that were represented mostly through clock gene transcripts (Fig.6C). There were further a
312 number of GO-terms associated with light perception like 'protein-chromophore linkage' and
313 'cellular response to light stimulus'. Transcripts significantly cycling only in rhythmic worms
314 showed enrichment for a variety of GO-terms with a notable accumulation of terms associated
315 with specific behaviors like 'neuromuscular process controlling balance' or 'mechanosensory
316 behavior' (Fig.6A,B). Further, these cycling transcripts showed an enrichment in metal ion
317 regulation processes (e.g. 'manganese ion homeostasis') and in GO-terms related to neuronal
318 differentiation such as 'regulation of long-term neuronal synaptic plasticity' and 'axon
319 regeneration' (Fig.6B), while similar terms were not enriched in transcripts cycling only in
320 arrhythmic worms (Fig.6D).

321 In arrhythmic worms, the number of transcripts with significantly diel cycling was
322 comparable to rhythmic worms (Fig.6A). This suggests that behavioral arrhythmicity does not
323 imply a generally lower rhythmicity on the level of physiology and gene expression.
324 However, the types of significantly cycling transcripts markedly differed from those of
325 behaviorally rhythmic worms. They showed an enrichment for GO-terms associated with
326 several metabolic pathways and cellular transport processes like 'fatty acid beta-oxidation
327 using acyl-CoA dehydrogenase', 'tricarboxylic acid metabolic process', and 'mitochondrial
328 transmembrane transport' (Fig.6D), highlighting that behavioral rhythmicity and
329 physiological rhythmicity do not necessarily correlate.

330 In addition to these "neuronal/behavioral" versus "metabolic" terms, there were several
331 GO-terms involved in the modification of the extracellular matrix such as 'collagen catabolic
332 process' (rhythmic worms), 'ossification' (arrhythmic worms) and 'extracellular matrix
333 disassembly' (both phenotypes). An investigation of the associated transcripts showed that
334 many encode for extracellular peptidases of the matrix metalloproteinase (MMP) family. We

335 next scanned all expressed transcripts (see methods) for potential MMPs, followed by
336 validation via BLASTx against the NCBI nr-database focusing on the characteristic ZnMc-
337 peptidase and hemopexin domains[53–55]. We were thereby able to identify at least 20 putative
338 *P. dumerilii* MMPs. Sequence matches for these MMPs in the *Platynereis* genome (Simakov
339 et al. in prep.) further confirmed that the respective transcripts derived from individual genes.
340 A total of 8 of the MMP transcripts showed RAIN-significant cycling in rhythmic worms
341 (n=3), arrhythmic worms (n=2) or both phenotypes (n=3) (Fig.6, Tab.S5).

342 For the heatmaps (Fig.6B-D), counts of a given transcript were normalized together
343 across rhythmic and arrhythmic worms in order to allow for a direct comparison of this
344 transcript between the different phenotypes. This plotting of the RAIN-significant transcripts
345 revealed that transcripts cycling in either rhythmic (Fig.6B) or arrhythmic worms (Fig.6D)
346 sometimes, but not always showed similar cyclic tendencies in the respective other phenotype
347 (Fig.6B-D). As illustrated by the heatmaps, the distinction by RAIN between cyclic and non-
348 cyclic expression was in many cases related to oscillation amplitudes. These differences in
349 amplitude could in principle arise in two ways. Scenario 1: Individual worms could still be
350 rhythmic for a given transcript over time, but the phases of this transcript would be less
351 synchronized across different worms. As we sampled multiple worm heads for each time
352 point, this would – due to averaging – result in a seemingly lowered amplitude or even the
353 loss of rhythmicity for a given transcript. Scenario 2: A given transcript could indeed oscillate
354 at lower amplitude or exhibit no diel oscillations in the respective phenotype.

355 The two scenarios should be discernable based on their variance. A reduction of phase
356 synchronization of transcript between different worms while maintaining amplitude (first
357 scenario) should result in an overall increased variance between biological replicates (i.e.
358 standard deviation). If the transcripts indeed cycle less in individual worms (second scenario),
359 the variance should overall not be affected across the different biological replicates. The
360 inspection of subgroups of transcripts significantly cycling only in rhythmic worms (GO-

361 terms related to behavior or neuronal processes) or only in arrhythmic worms (GO-terms
362 related to metabolism) showed that indeed both scenarios can be found (Fig.S4).
363

364 DISCUSSION

365 Behavioral individuality is ubiquitous in animals, but the molecular changes associated with
366 distinct phenotypes are still poorly understood. Here we uncovered diel behavior patterns of
367 the marine polychaete *Platynereis dumerilii*, which are individual-specific and persist over
368 time. Molecular analyses and mutant characterization reveal that the circadian clock and the
369 neuropeptide PDF are not or only partially responsible for rhythmic/arrhythmic behavioral
370 phenotypes, but that cyclic gene expression patterns show marked differences in
371 neuronal/behavioral versus metabolic transcripts with the latter showing stronger cycling in
372 behaviorally arrhythmic worms. Expression dynamics of extracellular matrix peptidases
373 further point towards a potential mechanism shaping phenotypic rhythmicity.
374

375 <u>The factors shaping rhythmic phenotype diversity</u>

376 The individual diversity in worm diel phenotypes is remarkable, especially given that many of
377 the investigated worms were siblings and raised together in the same culture boxes. The high
378 consistency of behavioral patterns over time illustrates that they are not just behavioral
379 snapshots of phenotypic plasticity, but individual characteristics. Similarly consistent
380 individual behavior patterns have been described in several other species[17,25] and in a striking
381 example Bierbach et al.[1] raised genetically identical freshwater fish under the exact same
382 conditions, but nevertheless observed individual-specific behavior patterns that persisted over
383 several rounds of investigations.

384 It is believed that individual phenotypes are realized either on the level of neuronal
385 organization and/or on the level of epigenetic modifications, based on predisposition or
386 (micro)environmental conditions[17,20,21,23,24]. As bet-hedging can induce stochastic epigenetic

387 diversity on the level of gametes [24], we can at present not discriminate whether the observed
388 *Platynereis* phenotypes result from genetic predisposition or rather epigenetic effects in
389 response to (micro)environmental conditions, or both [1,24,28].
390
391 The role of *pdf* in *P. dumerilii* diel rhythmicity
392 Pigment-dispersing factor (PDF) is seen as a neuropeptide central in regulating
393 *Drosophila* diel activity and coordination of the circadian clock neurons[56]. PDF has been
394 connected to temporal preferences of activity phases[21], the loss of rhythmicity after 2-3 days
395 of DD[3], and the light regime-dependent adjustment of diel activity patterns in drosophilid
396 species from different latitudes[33,57]. Our investigation of *pdf* worm mutants provides a new
397 functional perspective on this regulator from a very different animal group and ecological
398 context. As in *Drosophila melanogaster*[32,58,59], diel *pdf* expression does not cycle in *P.*
399 *dumerilii* and the loss of *pdf* does not directly affect the expression of the core circadian clock
400 genes. On the behavioral level, we find that loss of *pdf* can reduce diel rhythmicity, but in a
401 strain-dependent manner. The higher phenotypic diversity and overall higher rhythmicity of
402 PIN-strain compared to VIO-strain worms (Fig.1C,D) may suggest a higher capacity of the
403 PIN strain genetic background to compensate for *pdf* loss. In *Drosophila*, while most *pdf*
404 mutants become arrhythmic in DD, some individuals maintain circadian rhythmicity[3]. In the
405 light of the worm analyses, it will be interesting to compare the phenotypic consequences of
406 *pdf* loss between different strains and individuals in other species.
407
408 Transcript cycling patterns are largely clock-independent but phenotype-specific
409 An unanticipated finding was that wildtype worms characterized as rhythmic or arrhythmic
410 showed identical patterns for the circadian clock genes. This partly contrasts with the few
411 transcriptomic investigations of individual rhythmicity existing so far. Previous studies found
412 correlations between diel activity pattern and different circadian clock components in forager

413 versus nurse ants[26], as well as phenotype-specific expression of cryptochromes in zebrafish[25].
414 In *Drosophila*, while a transcriptome comparison of early/late emerging flies from different
415 strains found no difference in clock genes[27], phenotype differences in diel activity have been
416 linked to the clock gene *pdp*1 as well as the output genes *pdf* and *takeout*[21]. It should be noted
417 that we used whole heads while most *Drosophila* studies looked at specific brain regions or
418 neurons. Hence, phenotype-specific clock gene patterns on the level of individual neurons
419 cannot be fully excluded, although such patterns have not been seen so far[43].

420 The fact that worms that are behaviorally clearly rhythmic or arrhythmic show much
421 more nuanced differences in gene expression cycling further emphasizes that rhythmicity
422 determined on the behavioral level or through a limited number of candidate genes (e.g. clock
423 genes) is not necessarily representative of overall rhythmicity. This is especially highlighted
424 by the considerable number of transcripts cycling exclusively in behaviorally arrhythmic
425 worms. As physiology can – much like behavior – be very much individual-specific[60], our
426 results suggest that chronobiological phenotype investigations should be more routinely
427 complemented with high-throughput molecular approaches.

428 The enriched GO-terms associated with transcript that only cycle in either rhythmic or
429 arrhythmic worms likely reflect the differences in the respective lifestyles. For rhythmic
430 worms, the cycling of transcripts annotated to be linked to behaviors like 'righting reflex' and
431 flight behavior as well as neuronal plasticity suggests an overall higher responsiveness and
432 adaptability to the environment. This could benefit an explorative lifestyle in a food poor
433 habitat with regular foraging excursions that require and assessment of the surroundings and
434 potential predation risk. In contrast, the enrichment of metabolism-related GO-terms in
435 arrhythmic worms could represent the adjustment to a habitat where food readily available
436 (e.g. the surface of a kelp leaf). Under these conditions, no major excursions are necessary
437 and physiology could be optimized towards nutrient processing and growth.

438 The observation that behaviorally arrhythmic worms show enhanced metabolic
439 rhythmicity (relative to behaviorally rhythmic worms) again illustrates that behavioral output
440 alone may not be representative and that integrative investigations of biological rhythmicity
441 can be highly beneficial in revealing unexpected rhythmic complexity in any species.
442
443 Matrix metalloproteinases as potential mediators of rhythmic diversity
444 Our finding that transcripts of 8 of the 20 identified putative matrix metalloproteinases
445 (MMPs) showed phenotype-specific cyclic expression highlights these enzymes as interesting
446 factors for rhythmicity. MMPs are endopeptidases that are involved in the disassembly of
447 extracellular matrix proteins, thereby contributing several aspects of tissue development[53,54].
448 They play a major role in neuronal development and plasticity[55], and have been linked
449 specifically to motor axons in *Drosophila*[54,61,62]. Notably, the number of 20 *Platynereis*
450 MMPs exceeds those in *Drosophila melanogaster* (2 MMPs) and *Caenorhabditis elegans* (6
451 MMPs), and resembles those numbers found in zebrafish, the frog *Xenopus laevis* and a sea
452 urchin[54]. It is currently unknown, if this might reflect a general trend for higher MMP
453 numbers in aquatic species. One existing link between MMPs and rhythmicity is provided by
454 *Drosophila* MMP1 that can degrade PDF in clock neurons and is involved in circadian axonal
455 remodeling, with both overexpression and knockdown resulting in overall reduced activity
456 and partial arrhythmicity[4]. Circadian neuronal and vascular modifications based on MMPs
457 were also described in mammals[63,64].
458 Consistent with a deeper conservation of such mechanisms, a differential expression of
459 MMPs and associated differences in diel neuronal remodeling could be partially responsible
460 for the behavioral differences between rhythmic and arrhythmic worms. This is in line with
461 the cycling of *mef2* (transcript TRINITY_DN2510_c0_g1) in both phenotypes, as the gene is
462 under circadian control in *Drosophila* where it is also involved in neuronal development and
463 diel axonal remodeling of clock neurons [65].

464 Phenotype-specific expression of MMPs and associated neuronal remodeling could
465 present one way in which behavioral diversity is realized on the molecular/neuronal level.
466 MMPs thus present promising targets for investigations on how behavioral diversity and
467 rhythmic phenotypes are determined within individuals. Investigations of MMP-patterns may
468 also help explaining differences in diel rhythmicity patterns across species and
469 habitats[32,33,35,66].
470
471 Ecological benefits of phenotypic diversity – beyond the individual
472 Individual-specific phenotypes are not only advantageous for single animals, but may also
473 improve the overall fitness and resilience of populations and ecosystems. The offspring of
474 marine broadcast spawners like *P. dumerilii* spend their first life phase as part of the plankton
475 getting dispersed by currents, meaning they have limited influence on where they can settle
476 on the seafloor. A diversity of lifestyles can increase the chances of survival in heterogeneous
477 habitats and can help securing the persistence of the population. Phenotypic diversity can
478 further reduce competition due to a diversification of resource usage and spatial/temporal
479 niches[67,68]. Distinct individual phenotypes may be more beneficial in heterogeneous or
480 variable habitats like coral reefs, intertidal shores, forest or urban areas that provide a higher
481 potential for different lifestyles[22,69]. In contrast, in homogenous habitats like the open ocean
482 or grasslands, individual diversity may still be beneficial as it could prevent predators from
483 optimizing their foraging strategies and could also make populations more resilient to changes
484 of environmental parameters[70].
485 Individual diversity is an important factor to consider when determining tolerance
486 ranges to environmental conditions. Tolerance ranges are commonly reported as averages or
487 50% lethality limits for entire populations or species. Our transcriptome analysis shows that
488 rhythmic/arrhythmic individual phenotypes are associated with different physiological
489 adjustments, and physiological patterns in general can be individual-specific[60]. This likely

also affects the individual tolerance ranges for environmental conditions. Furthermore, patterns of behavioral rhythmicity can directly determine the conditions experienced by an animal[71]. Thus, a careful assessment of how many individuals one investigates, and how these are selected, is important to properly cover the individual diversity extant within a given group. This will help to make realistic predictions about a species' or population's tolerance windows. Exploring phenotypic diversity of behavior and physiology can thus also advance understanding of population-level responses to changing environmental conditions.

Conclusions

We identify extensive and consistent diel behavioral diversity among *P. dumerilii* strains and individuals which is correlated with several unanticipated observations. Individuality is a trait commonly associated only with 'higher' vertebrates. However, it is also a common behavioral feature in 'simple' invertebrates[17]. We find that on the rhythmic behavioral level, individual *Platynereis* worms can be discriminated based on their reproducible behavioral patterns.

The power of the behavioral rhythmic phenotypes is independent of the power of core circadian clock transcript cycling and, in contrast to *Drosophila*[56], genetic ablation of the neuropeptide PDF has no consistent effects in *P. dumerilii*. Our results argue that circadian rhythmicity can neither be defined through stereotypic behavioral phenotypes nor indicator genes alone, but that it is the sum of various processes acting on different levels of organization. Most notably, our observation of enhanced rhythmicity of metabolic transcripts in behaviorally arrhythmic worms highlights the complex relationship between the circadian clock and its behavioral and physiological outputs. We further find indications for a possibly conserved role of MMPs in the regulation of circadian clock output and diel rhythmic phenotypes, and find a general expansion of MMP numbers, which might be a shared feature in aquatic species. Investigating the factors that shape phenotypic and rhythmic diversity will help to understand how animals adapt to specific (micro)habitats and how these factors can

516 contribute to overall population fitness and ecosystem resilience. It highlights the importance
517 of treating biological variation not as 'background noise', but as an additional aspect of
518 biodiversity that needs to be considered for the mechanistic and the ecological context[16,72].
519

520 # MATERIAL & METHODS

521 ## Table of resources

REAGENT or RESOURCE	SOURCE	IDENTIFIER
Chemicals, peptides, and recombinant proteins		
OneTaq® 2X Master Mix	New England BioLabs, USA	M0482S
RNAzol® RT	Sigma-Aldrich, USA	R4533
Synthetic amidated PDF peptide for deorphanization (sequence: NH2-NPGTLDAVLDMPDLMSL-COOH)	this paper	N/A
pdf fwd TALEN (RVDs: NI-NI-NG-NN-NG-NN-NN-NI-NG-NG-NG-HD-NI-NI-NI-NN-HD)	this paper	N/A
pdf rev TALEN (RVDs: HD-HD-NI-NN-NG-NN-NG-NN-HD-HD-NI-NN-NN-NN-NG-NG-NN)	this paper	N/A
Critical commercial assays		
Direct-Zol RNA MiniPrep kit	Zymo Research, USA	R2052
LunaScript® RT SuperMix kit	New England BioLabs, USA	205313
Luna® Universal qPCR Master Mix	New England BioLabs, USA	M3003S
GelGreen® Nucleic Acid Gel Stain	Biotium, USA	41005
NEBNext® Multiplex Oligos for Illumina®	New England BioLabs, USA	E6440S
Deposited data		
Individual actograms of *P. dumerilii* strain comparison	this paper	please contact authors
Individual actograms of *P. dumerilii pdf* wildtype vs. mutant comparison	this paper	please contact authors
Individual actograms of *P. dumerilii* behavioral characterization	this paper	please contact authors
P. dumerilii tail reference transcriptome for mapping	this paper	please contact authors
.fastq-files with trimmed forward and reverse reads (2 files/sample)	this paper	please contact authors
.fastqc-files with quality report for trimmed .fastq-files	this paper	please contact authors
Experimental models: Cell lines		
Chinese hamster ovary (CHO) cells	PerkinElmer, Belgium	ES-000-A2
E. coli competent cells (XL1-blue)	Tessmar-Raible group, Max Perutz Labs	N/A
Experimental models: Organisms/strains		
P. dumerilii PIN strain	Zantke et al. 2014[45]	N/A

P. dumerilii VIO strain	Zantke et al. 2014[45]	N/A
P. dumerilii NAP strain	Zantke et al. 2014[45]	N/A
P. dumerilii pdf$^{14/-14}$ mutant strain	this paper	N/A
P. dumerilii pdf$^{+4/+4}$ mutant strain	this paper	N/A
Oligonucleotides		
pdf genotyping primers fwd: 5'- GCGCTATGCTGCAAAAATAGCTCGC-3' rev: 5'- CGAGGGACATAAGGTCGGGCAT-3'	this paper	N/A
pdfr cloning primers fwd: 5'-GCTAAGCTTGCCACCATGCACGCCCTTCC-3' rev: 5'-GGCTCTAGATCACCCCCCTGGACGTTGGTCAC-3'	this paper	N/A
bmal qPCR primers fwd: 5'- TCCGATTTATCTCCACGAGAA-3' rev: 5'- TCCGTCTTTACAGGCAGCA-3'	Veedin-Rajan et al. 2021[39]	N/A
per qPCR primers fwd: 5'-GGTCAACATGAAGTCGTACAGG-3' rev: 5'- CACTGGTTTTCGGCTCAAG-3'	Veedin-Rajan et al. 2021[39]	N/A
trcry qPCR primers fwd: 5'- TGTTCAAATTCCATGGGACA-3' rev: 5'- TGTTTTAGCCTCAGCCCATT-3'	Veedin-Rajan et al. 2021[39]	N/A
cdc5 qPCR primers fwd: 5'- CCTATTGACATGGACGAAGATG-3' rev: 5'- TTCCCTGTGTGTTCGCAAG-3'	Veedin-Rajan et al. 2021[39]	N/A
Recombinant DNA		
pCDNA3.1(+) cloning vector	Thermo Fisher Scientific, USA	V79020
pjet1.2 blunt vector (CloneJET™ PCR Cloning Kit)	Thermo Fisher Scientific, USA	K1231
pGEM®-T Easy Vector (pGEM®-T Easy Vector Systems Kit)	Promega, USA	A1360
Software and algorithms		
RStudio v.1.1.453	R Development Core Team 2013[75]	https://www.r-project.org
R-package 'DESeq2' v.1.30.1	Love et al. 2014[76]	https://bioconductor.org/packages/DESeq2/
R-package 'RAIN' v.1.24.0	Thabe & Westermark 2014[51]	https://bioconductor.org/packages/rain/
R-package 'topGO' v.2.46.0	Alexa & Rahnenführer 2009[77]	https://bioconductor.org/packages/topGO/
R-package 'gplot' v.3.1.1	Warnes et al. 2016[78]	https://CRAN.R-project.org/package=gplots
R-package 'RColorBrewer' v.1.1-2	Neuwirth 2014[79]	https://CRAN.R-project.org/package=RColorBrewer
ImageJ/Fiji v.1.52d	Schindelin et al. 2012[80]	https://imagej.nih.gov/ij/index.html
ActogramJ v.1.0	Schmid et al. 2011[81]	https://bene51.github.io/ActogramJ/
StepOne v.2.3 Software for qPCR analysis	Thermo Fisher Scientific, USA	https://www.thermofisher.com
salmon v.1.4	Patro et al. 2017[82]	https://combine-lab.github.io/salmon/

SAMtools v.1.3.1	Li et al. 2009[83]	http://samtools.sourceforge.net
cutadapt v.1.12	Martin 2011[84]	https://cutadapt.readthedocs.io/en/stable/index.html
FastQC v. 0.11.9	Andrews 2010[85]	http://www.bioinformatics.babraham.ac.uk/projects/fastqc/
GraphPad Prism v.9.2.0	GraphPad Software, USA	https://www.graphpad.com
Adobe Illustrator v.25.3.1	Adobe, USA	https://www.adobe.com/at/products/illustrator.html
TransDecoder	Haas et al.	https://github.com/TransDecoder/TransDecoder
HMMER v.3.3.1	Mistry et al. 2021[86]	http://hmmer.org
Other		
Meersalz CLASSIC sea salt	Tropic Marine, Switzerland	10134
Organic Spirulina powder	Micro Ingredients, USA	SPA-0520
TetraMin fish flakes	Tetra GmbH, Germany	769939

522

523 **Contact for resource sharing**

524 Additional information of used reagents, sequence resources and bioinformatics analysis can
525 be requested from the corresponding authors Kristin Tessmar-Raible
526 (kristin.tessmar@mfpl.ac.at) and Sören Häfker (soeren_haefker@web.de).

527

528 **Experimental model & subject details**

529 We performed all investigations on the marine annelid *Platynereis dumerilii* (Audouin &
530 Milne Edwards, 1833). The worms used in the initial behavioral comparison of strains and
531 individuals (Fig.1) originated from 3 wildtype strains, which all originated from Worms
532 collected in the Gulf of Naples, Italy (40.7°N, 14.2E). The PIN and VIO strains have been in
533 culture for ~70 years and have been incrossed at least 10 times[40,45]. The NAP strain was
534 established in 2009 and has been kept as non-incrossed closed culture at Max Perutz Labs
535 (Vienna, Austria). p*df* mutants and were generated in VIO worms with corresponding

536 wildtypes obtained from the same heterozygous worms. Later, mutants were crossed into the
537 PIN strain and the resulting mutants and corresponding wildtypes were used for additional
538 behavior experiments (Fig.3A,B, Fig.4). qPCR measurement were performed with worms
539 from a VIO background (Fig.3C-E) For the comparison of rhythmic/arrhythmic worms
540 (Fig.5,6) we used only PIN worms. For all experiments we used only immature/premature
541 worms (age: 3-7 months, min. length: ~2.5 cm) that did not show any signs of metamorphosis
542 to the adult (epitoke) form.
543
544 **Method details**
545 Worm culture conditions
546 All worms used in the described experiments were cultured at the Max Perutz Labs (Vienna,
547 Austria) in a 1:1 mix of natural and artificial seawater (Meersalz CLASSIC, Tropic Marine
548 AG, Switzerland) that was pumped through 1 µm filters before use and was exchanged at
549 least every 2 weeks. Worms were kept in transparent plastic boxes (30x20 cm, 100-150
550 indv./box) in temperature controlled rooms at 19.5±1.0°C under a rectangular 16h:8h
551 light/dark-cycle (LD) with fluorescent tubes ($4.78*10^{14}$ photons*cm^{-2}*s^{-1}, Master TL5 HO
552 54W/865, Philips, Netherlands, Fig.S1A,C). To account for *P. dumerilii*'s lunar reproductive
553 cycle[43,87,88], we simulated a moonlight cycle by an LED lamp (Warm White 2700K A60 9W,
554 Philips, Netherlands) that was switched on for 8 nights centered on the outdoor full moon
555 times (see Zurl et al. 2022[44] for details). Larvae worms were fed a mix of living *Tetraselmis*
556 algae and *Spirulina* (Organic Spirulina Powder, Micro Ingredients, USA) 2-3 times a week
557 until they started forming their living tubes. Thereafter, worms were fed shredded spinach and
558 powdered fish flakes (TetraMin, Tetra GmbH, Germany) (once a week, each). Under these
559 conditions, *P. dumerilii* has a generation time of min. 3 months.
560

561 Recording and characterization of behavior and diel rhythmicity

562 We investigated worm locomotor activity in light-tight chambers developed in cooperation
563 with loopbio GmbH, Austria[39,89]. The worms were last fed (spinach) 4 days before the start of
564 the investigation. Worms were always taken from culture boxes of similar animal densities
565 and age to avoid potential effect on behavior. To prevent potential behavioral changes
566 associated with the simulated lunar cycle (see above), we conducted all recordings in the 2
567 weeks around new moon. For recording, the worms were transferred to 5x5 well plates and
568 were filmed at 15 fps using infrared-illumination and a camera equipped with a long-pass IR-
569 filter (acA2040-90um, Basler AG, Germany). A custom-build LED-array was used to create a
570 natural 16h:8h LD-cycle ($1.40*10^{15}$ photons*cm^{-2}*s^{-1}, Marine Breeding Systems GmbH,
571 Switzerland, Fig.S1B,C). All recordings were done at culture temperature and diel oscillations
572 were ~1°C in LD and <0.5°C in constant darkness (DD).

573 The number of days in LD or DD depended on the specific investigation. For the
574 comparison of the PIN, NAP and VIO wildtype strains (Fig.1), we exposed the worms to 4
575 days of LD followed by 4 days of DD. Worms in the comparison of *pdf* mutants and
576 wildtypes (Fig.4) experienced 4 LD days followed by 4, 5 or 8 DD days. The fractions of
577 worms experiencing a give number of DD days did not differ between wildtypes and mutants.
578 During the characterization for RNASeq analysis (Fig.5,6) we exposed PIN strain wildtypes
579 to 3 LD days and 3 DD days. Actograms of individual worms used in strain comparison, *pdf*
580 wildtype/mutant comparison, and characterization for RNASeq were submitted to Dryad
581 (Fig.D1-3).

582 We excluded data from worms that matured/spawned during or within one week after
583 the recording. Data of worms that crawled out of the well and could no longer be recorded
584 were omitted, if less than 3 days of data were available for the respective recoding phase (LD
585 or DD). Worms that were recorded repeatedly were kept separately in smaller boxes after the
586 initial recording to avoid the confusion of individuals. The *pdf* genotypes of all mutants and

587 the associated wildtype worms were verified at least 1 month before the behavior recording or
588 directly afterwards (as described below). Sex determination in a limited number of wildtype
589 worms showed no consistent differences in locomotor behavior of males and females (Fig.D1
590 in Dryad).

591 We quantified locomotor activity by determining x/y-coordinates of the center of the
592 detected worm shape (Fig.5A) and measuring the distance moved between frames using the
593 Motif automated tracking software (loopbio GmbH, Austria, see Veedin-Rajan et al.[39] for
594 details). We used a 1-min moving average to reduce noise. Period and power of diel
595 rhythmicity was determined via Lomb-Scargle periodograms with the ActogramJ[81] plug-in in
596 ImageJ/Fiji[80]. Analysis focused on the 20h-28h range of diel/circadian rhythmicity. Overall
597 activity was binned into morning (ZT0-8), afternoon (ZT8-16) and night (ZT16-0) for the LD
598 phase and into subjective morning (circadian time, CT0-8), subjective afternoon (CT8-16)
599 and subjective night (CT16-0) for the DD phase with all days of the respective phases being
600 pooled.

601

602 Description of *P. dumerilii* pigment-dispersing factor (*pdf*) and receptor (*pdfr*) sequences

603 An initial *P. dumerilii pdf* gene fragment was identified from Expressed Sequence Tags
604 (ESTs)[73]. The resulting 567bp fragment was subsequently extended to 804bp, which included
605 the complete coding sequence (CDS) of the prepropetide (accession no°: GU322426.1).

606 A first fragment of the *P. dumerilii* PDF-receptor (*pdfr*) sequence was obtained by
607 degenerated PCR and subsequently extended by RACE-PCR[74]. A 1604bp sequence
608 containing the full CDS was cloned into a pGEM®-T Easy Vector (pGEM®-T Easy Vector
609 Systems Kit, Promega, USA) and sequenced (accession no°: OL606759). A draft genome of
610 *P.dumerilii* (Simakov et al. in prep.) was searched for possible gene duplicates of *pdf* using a
611 hidden Markov model, but no further copies were identified. For the construction of
612 phylogenetic trees for prepro-PDF and PDF-receptor (Fig.2A,B), we collected sequences

613 from NCBI via PSI-BLAST (3 iterations), aligned them with MUSCLE[90] and then
614 constructed the trees using the IQ-TREE online tool with default settings[91]. Sequences used
615 for tree construction are provided in the supplement (Tab.S1).
616
617 Deorphanization of pigment-dispersing factor receptor
618 To validate that the identified *pdfr* sequence encodes a functional receptor activated by PDF,
619 a fragment of the *pdfr* gene including the full coding sequence was amplified by PCR and
620 cloned into the HindIII/XbaI sites of the pCDNA3.1(+) cloning vector. We assessed receptor
621 activation as previously described[48]. Briefly, *pdfr*-transfected Chinese Hamster Ovary (CHO)
622 cells expressing *apoaequorin* and the *human Gα16 subunit* were incubated with 10^{-13}-10^{-4} M
623 of synthetic amidated PDF (see Key Resource Table) with n=10-12 measurements per
624 concentration. PDF was provided by the Mass Spectrometry Facility of the Institute for
625 Molecular Pathology, Vienna; and assessed by the Chemistry Department of the University of
626 Vienna for purity using matrix-assisted laser desorption/ionization time-of-flight mass
627 spectrometry (MALDI-TOF-MS). We recorded calcium responses for 30 sec using a Mithras
628 LB 940 luminometer (Berthold Technologies, Germany). After these ligand-stimulated
629 calcium measurements, Triton X-100 (0.1%) was added to each sample well to obtain a
630 measure of the maximum calcium response and calculate dose responses. Percentage
631 activation values were plotted, with cells transfected with an empty pCDNA3.1(+) vector
632 serving as negative controls with n=6 per concentration (Fig.2C, Tab.S2). The half-maximal
633 effective concentration (EC_{50}) was calculated using a computerized nonlinear regression
634 analysis with a sigmoidal dose–response equation using GraphPad Prism (GraphPad Software
635 Inc., USA).
636

637 Generation of *pdf*-mutant strain using TALENs

638 To achieve a knockout of the *P. dumerilii pdf* gene, we followed a reverse genetic approach
639 using TALENs (transcription activator-like effector nucleases) as previously described[49].
640 Repeat-variable di-residue (RVD) sequence of TALENs were designed based on the
641 previously identified *pdf* sequence (accession nr: GU322426.1) to target a site in the 3rd exon
642 preceding the start of the mature peptide sequence (see Key Resource Table). VIO strain
643 worm zygotes 1 hour post fertilization were digested with proteinase K (23 sec) and were then
644 injected with 10 µL injection solution, which consistent of 200 ng/µL of each TALEN, 8 µL
645 RNAse-free H_2O and 2 µL TRITC-dextrane (3% in 0.2 M KCl). Before injection, the solution
646 was filtered through 0.45 mm PVDF centrifugal filters (Ultrafree-MC-HV, Merck Millipore,
647 USA)[49].

648 Once grown to maturity, we outcrossed injected worms against VIO wildtype worms,
649 and the resulting offspring were genotyped to identify changes in the PCR-product length of
650 the *pdf* locus using the HotSHOT-method[92] and primers covering the TALENs cleavage site.
651 PCR products were run on agarose gels[93]. When changes in length compared to the wildtype
652 were found, the bands were cut out and sub-cloned according to manufacturer protocols into
653 either a pjet1.2 blunt vector (CloneJET™ PCR Cloning Kit, Thermo Fisher Scientific, USA)
654 or a pGEM®-T Easy Vector (pGEM®-T Easy Vector Systems Kit, Promega, USA) depending
655 on the Taq-polymerase used for PCR (blunt vs. sticky ends). The vectors were used to
656 transform competent *E. coli* cells (XL1-blue, raised by lab technician), of which individual
657 colonies were picked. Success of the transformation was verified by PCR followed by
658 sequencing of the insert to identify base deletions/insertions[93]. We thereby established a -14bp
659 deletion mutant strain, a +4bp insertion mutant strain, as well as a corresponding wildtype
660 strain (Fig.3A). The mutations resulted in early stop codons and a complete loss of the mature
661 peptide sequence (Fig.2B). The strains were outcrossed against VIO wildtypes at least 3 times
662 before later also being crossed against PIN wildtypes.

663

664 qPCR measurements

665 After entrainment to a 16h:8h LD cycle, we sampled worm heads of *pdf* wildtypes and -14/-
666 14 mutants (both VIO background) on the 2nd day of constant darkness at circadian time (CT)
667 6, CT10, CT15, CT19 and CT24. For this, we anesthetized worms in 7.5% (w/v) $MgCl_2$
668 mixed 1:1 with sterile filtered seawater for 5 minutes and heads were cut before the first pair
669 of parapodia under a dissection microscope before being fixed in liquid nitrogen. Animals
670 were only briefly exposed to light during dissection. At each time point, 3 replicates of mutant
671 and wildtype worms were collected with 5 heads pooled per replicate (only 2 replicates for
672 ZT10).

673 For RNA extraction, we homogenized samples in 350 µL RNAzol® (Sigma-Aldrich, USA)
674 with a TissueLyser (Qiagen, Netherlands) for 2 min at 30Hz and extracted RNA using the
675 Direct-Zol RNA MiniPrep kit (Zymo Research, USA) with on-column DNA digest according
676 to the manufacturer protocol. RNA was eluded in 25µL Nuclease-free H_2O and was stored at -
677 80°C. We spectrometrically determined RNA concentration and purity (Nanodrop 2000,
678 Thermo Fisher Scientific, USA). 1 µg RNA was reverse transcribed to cDNA (LunaScript RT
679 SuperMix, New England BioLabs, USA).

680 We measured the expression of the circadian clock genes *brain and muscle Arnt-like*
681 *protein* (*bmal*), *period* (*per*) and *tr-cryptochrome* (*tr-cry*) via real-time qPCR
682 (StepOnePlus™, Applied Biosystems, USA) using previously established primers[39] and the
683 expression of *cell division cycle 5* (*cdc5*) acting as a reference[94] (Fig.3C-E, Tab.S3). All
684 samples were measured as technical duplicates.

685

686 Characterization and sampling for RNASeq analysis

687 To investigate the manifestation of differences in phenotypic rhythmicity on the transcriptome
688 level, we performed a total of 13 behavioral recordings (see above) over the course of 6
689 months using worms from 5 different mating batches. We characterized worms as rhythmic
690 (n=102) or arrhythmic (n=75) based on Lomb-Scargle periodogram analysis and visual
691 inspection of actograms. For the characterization, rhythmicity in DD was considered more
692 important than in LD. Worm that could not be clearly associated with one phenotype were
693 considered unclear and were not used further (n=148, includes maturing/spawning worms).
694 While the relative abundance of phenotypes did partially differ between recordings, all
695 included rhythmic and arrhythmic worms. Actograms of all individual worms including their
696 characterizations were submitted to Dryad (Fig.D3).

697 We sorted characterized worms to culture boxes based on phenotype and kept them
698 under standard conditions (LD 16h:8h + lunar cycle) until sampling at the next new moon (i.e.
699 ~1 month after the behavioral characterization). Samples for RNASeq analysis were collected
700 at ZT0 (lights on), ZT4, ZT8, ZT16 (lights off) and ZT20 (Fig.5A). Due to the work-intensive
701 characterization procedure and the loss of characterized worms due to maturation, we could
702 not collect all samples for the diel time series 'in one go', but sampled discontinuously over
703 several months while making sure that replicates of the same rhythmic phenotype/time point
704 were not collected simultaneously. Worm age at the time of sampling was 4-7 months. We
705 last fed the worms 5 days before sample collection and transferred them to sterile filtered
706 seawater containing 0.063 mg/mL streptomycin-sulfate and 0.250 mg/mL ampicillin 2 days
707 prior to sampling to minimize bacterial contaminations. Worms were anesthetized in $MgCl_2$
708 and heads were sampled and fixed as described above for qPCR measurements with 3 heads
709 pooled per replicate. For each time point, we collected 3 replicates of rhythmic and
710 arrhythmic worms, respectively. RNA was extracted as described above and was stored at -
711 80°C.

712

713 **Quantification & statistical analysis**

714 Behavioral comparisons

715 For the comparison of wildtype strains, we performed locomotor activity recordings of n=25
716 PIN worms, n=21 NAP worms and n=38 VIO worms (Fig.1 and Fig.D1 in Dryad). PIN, NAP
717 and VIO worms for the comparison originated from 2 mating batches, each. Of these,
718 repetition runs were done with 12 PIN worms, 5 NAP worms and 13 VIO worms (Fig.1E-G,
719 Fig.S2). For the behavioral comparison of *pdf* mutants and wildtypes, we performed 4
720 locomotor recordings for VIO-worms (wildtype n=34 from 4 batches & *pdf* -/- n=43 from 5
721 batches) and 5 recordings for PIN-crossed worms (wildtype n=45 from 5 batches & *pdf* -/-
722 n=54 from 6 batches). The VIO mutants were genotypes were -14/-14 (n=33) and -14/+4
723 (n=10). The PIN-crossed mutant genotypes were -14/-14 (n=16), +4/+4 (n=31) and -14/+4
724 (n=7). As the mutants showed no within-strain differences among genotypes (Fig.D2 in
725 Dryad), all of mutants with the same strain background were pooled.

726 We compared of diel rhythmicity power between groups, as well as activity between
727 time bins and between groups (see above) via 2-side unpaired Student's t-test or via One-way
728 ANOVA with Holm-Sidak *post-hoc* test. If data were not normally distributed and/or
729 homoscedasticity of variances was not given, we replaced the t-test with a Mann-Whitney U-
730 test and the One-way ANOVA with a Welch's ANOVA with Dunnett-T3 *post-hoc* test or a
731 Kruskal-Wallis ANOVA on Ranks with Dunn's *post-hoc* test. All statistical analyses were
732 carried out in GraphPad Prism.

733

734 Analysis of qPCR data

735 We normalized raw C_T-values of the clock genes *bmal*, *per* and *tr-cry* according to the $2^{-\Delta\Delta CT}$-
736 Method[95] using the gene *cdcd5* as a reference (Fig.3C-E). Expression stability of *cdc5* has
737 previously been verified[94]. Raw C_t-values are provided in the supplement (Tab.S3).

738 Differences between worm groups were analyzed using GraphPad Prism via Student's t-tests
739 for each time point and with correction for the testing of multiple time points.
740
741 Processing of RNASeq data
742 Quality control, reverse transcription and library preparation of rhythmic/arrhythmic samples
743 were performed by the VBCF Next-Generation Sequencing facility services according to
744 standard procedures (VBCF-NGS, Vienna Biocenter Campus,
745 https://www.viennabiocenter.org/vbcf/next-generation-sequencing). Samples were run on a
746 NextSeq550 System (Illumina, USA) with the High Output-kit as 75bp paired-end reads and
747 resulted in a total of 445,553,522 raw reads (sample range: 9,973,579-15,234,688 reads).
748 We trimmed/filtered the raw reads from NextSeq sequencing (see above) using cutadapt
749 (--nextseq-trim=20 -m 35 --pair-filter=any) with adapters being remove in the process[84]. This
750 reduced read numbers to 443,393,107 reads (0.48% loss). Read quality was checked before
751 and after trimming using FastQC[85]. Trimmed reads were mapped against a *P. dumerilii*
752 reference transcriptome generated from regenerated tail pieces (Fig.5B). Trimmed-read fastq-
753 files and FastQC-reports as well as transcript sequences of the reference transcriptome were
754 submitted to Dryad. We chose this tail transcriptome, because a BUSCO analysis[96] showed
755 that it contained a higher percentage of near-universal single-copy orthologs (98.9%
756 complete) compared to a previously published transcriptome generated from worm heads[94].
757 To ensure that no important transcripts were lost due to tissue-dependent expression, we
758 manually verified the inclusion of known clock genes, opsins, neuropeptides and other
759 potential genes of interest. The respective transcripts were identified using internal sequence
760 resources and NCBI, and were verified via BLASTx against the nr-database. If sequences
761 from existing resources covered larger gene stretches than the respective transcript, we
762 replaced the sequences in the transcriptome or merged them. Trimmed reads were mapped to
763 the reference transcriptome using salmon tool[82] (standard parameters incl. multi-mapping,

764 library type: ISR). To exclude transcripts that did not receive any reads during mapping, we
765 removed those transcripts from the expression matrix that had no observed expression in at
766 least 2 time points in the rhythmic time as well as the arrhythmic samples. We further
767 excluded all transcript <500bp to avoid fragments that could not be reliably annotated,
768 thereby obtaining a total of 48,605 expressed transcripts (Fig.5B, Tab.S4).
769
770 Identification of cycling transcripts with RAIN
771 To identify cyclic changes in transcript expression patterns, we used the R-package 'RAIN',
772 which employs a non-parametric approach to identify cycling independent of waveform[51]. As
773 RAIN assumes homoscedasticity, raw count data were transformed via the
774 *VarianceStabilizingTransformation* function of the DESeq2 package prior to analysis[76].
775 Cycling was investigated separately for rhythmic and arrhythmic samples with
776 peak.border=c(0.3,0.7) for a 24h period. We could not test for other periods due to the
777 discontinuous sample collection, which would have disrupted non-24h cycles (see above).
778 Resulting p-values were false-discovery-rate corrected via the *p.adjust()* function in R
779 according to the Benjamini-Hochberg-procedure[97] with p-values <0.05 considered significant
780 (Fig.6A, Tab.S4).
781 For visualization, we normalized VST-counts of RAIN-significant transcripts to a scale
782 of -1 to 1 and plotted them in heatmaps using the R-package *gplots*[78] and *RColorBrewer*[79].
783 Transcripts with cycling in rhythmic worms, arrhythmic worms, or both were plotted
784 separately, but always for both phenotypes (Fig.6B-D). The normalization means that
785 expression amplitudes of a given transcript are comparable between rhythmic and arrhythmic
786 worms, but not between different transcripts or groups (rhythmic, arrhythmic, both).
787

788 GO-term annotation and enrichment analysis

789 We next performed Gene Ontology (GO) analysis to determined the enrichment of biological
790 processes among transcripts with RAIN-significant cycling. For this, transcripts were
791 assigned GO-terms using the Trinotate protocol[98]. Briefly, we used TransDecoder
792 (https://github.com/TransDecoder/TransDecoder) to identify the most likely longest open
793 reading frame (ORF) peptide candidates and performed a BLASTx or BLASTp search of the
794 transcripts or peptide candidates against the SwissProt database (UniRef90)[99,100].
795 Additionally, we used the *hmmscan* function from HMMER (v3.3.1, http://hmmher.org/) to
796 get functional information from protein domains by searching the Pfam database[86]. For
797 analysis we pooled the GO-terms hits that had e-values $<1*10^{-3}$ in any of the annotation
798 approaches. GO-terms could be assigned to 19,096 out of the 48,605 expressed transcripts,
799 and to 334, 273 and 176 of the transcripts cycling in rhythmic, arrhythmic and both
800 phenotypes, respectively.

801 We determined GO-term enrichment for cycling transcripts using the R-package
802 'topGO'[77], using Fisher's exact test and the 'elim' algorithm[77,101]. The elim algorithm avoids
803 redundant scoring of more general GO-terms and thereby gives higher significance to more
804 specific terms than the 'classic' algorithm. GO-terms were considered significantly enriched,
805 if they had a p-value ≤ 0.05 and were represented by at least 3 transcripts (Fig.6B-D).

806

807 **DATA AND CODE AVAILABILITY**

808 All data relevant to the paper are provided in the supplemental material or were submitted to
809 Dryad (figures included in supplement, for transcriptomic data please contact the authors). No
810 custom code was used. For additional information, please contact the authors directly
811 (kristin.tessmar@mfpl.ac.at, soeren_haefker@web.de).

812

COMPETING INTERESTS

The authors declare no competing interests.

ACKNOWLEDGMENTS

N.S.H. was supported by a Lise-Meitner fellowship by the Austrian Science Fund (FWF, M2820). K.T.-R. received funding from the European Research Council under the European Community‘s Seventh Framework Programme (FP7/2007–2013) ERC Grant Agreement #337011, the Horizon 2020 Programme ERC Grant Agreement #819952, and the FWF research platform ‘Rhythms of Life’ of the University of Vienna (SFB F78). I.B and L.S received support from the KU Leuven Research Council (C16/19/003). F.R. acknowledges support by the FWF (#I2972), and the European Research Council (#260564). None of the funding bodies was involved in the design of the study, the collection, analysis, and interpretation of data or in writing the manuscript.

We are further grateful to Andrij Belokurov, Margaryta Bosysova and Netsaneh Getachew (Max Perutz Labs Aquatic Facility) for sustaining worm cultures and routine genotyping support.

AUTHOR CONTRIBUTIONS

N.S.H. and K.T.-R. designed the study and interpreted the results. N.S.H. wrote the manuscript with comments by K.T.-R. and review by the other coauthors. N.S.H. performed investigations of locomotor activity and phenotype characterization. S. H. identified the *pdf* gene sequence. K.V. generated *pdf* mutants and performed clock gene qPCRs. I.B., K.V. and L.S. performed deorphanization of the PDF-receptor. N.S.H. collected and prepared samples for transcriptomics. N.S.H., F.R. and A.W.S. preprocessed transcriptome data and A.W.S. assembled the reference transcriptome used for mapping. L.H. performed GO-term annotation and analysis, and N.S.H. performed RAIN analysis.

839

840 **REFERENCES**

841 1. Bierbach, D., Laskowski, K.L., and Wolf, M. (2017). Behavioural individuality in clonal
842 fish arises despite near-identical rearing conditions. Nat. Commun. *8*, 15361.

843 2. Refinetti, R., Wassmer, T., Basu, P., Cherukalady, R., Pandey, V.K., Singaravel, M.,
844 Giannetto, C., and Piccione, G. (2016). Variability of behavioral chronotypes of 16
845 mammalian species under controlled conditions. Physiol. Behav. *161*, 53–59.

846 3. Renn, S.C.P., Park, J.H., Rosbash, M., Hall, J.C., and Taghert, P.H. (1999). A *pdf*
847 Neuropeptide Gene Mutation and Ablation of PDF Neurons Each Cause Severe
848 Abnormalities of Behavioral Circadian Rhythms in *Drosophila*. Cell *99*, 791–802.

849 4. Depetris-Chauvin, A., Fernández-Gamba, Á., Gorostiza, E.A., Herrero, A., Castaño,
850 E.M., and Ceriani, M.F. (2014). Mmp1 Processing of the PDF Neuropeptide Regulates
851 Circadian Structural Plasticity of Pacemaker Neurons. PLOS Genet. *10*, e1004700.

852 5. Tessmar-Raible, K., Raible, F., and Arboleda, E. (2011). Another place, another timer:
853 Marine species and the rhythms of life. BioEssays *33*, 165–172.

854 6. Häfker, N.S., Andreatta, G., Manzotti, A., Falciatore, A., Raible, F., and Tessmar-Raible,
855 K. (accepted). Rhythms and Clocks in Marine Organisms. Annu. Rev. Mar. Sci.

856 7. Mat, A.M., Sarrazin, J., Markov, G.V., Apremont, V., Dubreuil, C., Eché, C., Fabioux, C.,
857 Klopp, C., Sarradin, P.-M., Tanguy, A., et al. (2020). Biological rhythms in the deep-sea
858 hydrothermal mussel *Bathymodiolus azoricus*. Nat. Commun. *11*, 3454.

859 8. Aguzzi, J., Sbragaglia, V., Tecchio, S., Navarro, J., and Company, J.B. (2015). Rhythmic
860 behaviour of marine benthopelagic species and the synchronous dynamics of benthic
861 communities. Deep Sea Res. Part Oceanogr. Res. Pap. *95*, 1–11.

862 9. Kelly, L.W., Nelson, C.E., Haas, A.F., Naliboff, D.S., Calhoun, S., Carlson, C.A.,
863 Edwards, R.A., Fox, M.D., Hatay, M., Johnson, M.D., et al. (2019). Diel population and
864 functional synchrony of microbial communities on coral reefs. Nat. Commun. *10*, 1691.

865 10. Bandara, K., Varpe, Ø., Wijewardene, L., Tverberg, V., and Eiane, K. (2021). Two
866 hundred years of zooplankton vertical migration research. Biol. Rev. *96*, 1547–1589.

867 11. Häfker, N.S., and Tessmar-Raible, K. (2020). Rhythms of behavior: are the times
868 changin'? Curr. Opin. Neurobiol. *60*, 55–66.

869 12. Dunlap, J.C., and Loros, J.J. (2016). Yes, circadian rhythms actually do affect almost
870 everything. Cell Res. *26*, 759–760.

871 13. Mackey, S.R. (2007). Biological Rhythms Workshop IA: Molecular Basis of Rhythms
872 Generation. In Cold Spring Harbor Symposia on Quantitative Biology (Cold Spring
873 Harbor Laboratory Press), pp. 7–19.

874 14. Horn, M., Mitesser, O., Hovestadt, T., Yoshii, T., Rieger, D., and Helfrich-Förster, C.
875 (2019). The Circadian Clock Improves Fitness in the Fruit Fly, *Drosophila melanogaster*.
876 Front. Physiol. *10*, 1374.

877 15. Spoelstra, K., Wikelski, M., Daan, S., Loudon, A.S.I., and Hau, M. (2016). Natural
878 selection against a circadian clock gene mutation in mice. Proc. Natl. Acad. Sci. *113*,
879 686–691.

880 16. Dall, S.R.X., Bell, A.M., Bolnick, D.I., and Ratnieks, F.L.W. (2012). An evolutionary
881 ecology of individual differences. Ecol. Lett. *15*, 1189–1198.

882 17. Kralj-Fišer, S., and Schuett, W. (2014). Studying personality variation in invertebrates:
883 why bother? Anim. Behav. *91*, 41–52.

884 18. Demin, K.A., Lakstygal, A.M., Alekseeva, P.A., Sysoev, M., de Abreu, M.S., Alpyshov,
885 E.T., Serikuly, N., Wang, D., Wang, M., Tang, Z., et al. (2019). The role of intraspecies
886 variation in fish neurobehavioral and neuropharmacological phenotypes in aquatic
887 models. Aquat. Toxicol. *210*, 44–55.

888 19. Mueller, J.C., Korsten, P., Hermannstaedter, C., Feulner, T., Dingemanse, N.J.,
889 Matthysen, E., Oers, K. van, Overveld, T. van, Patrick, S.C., Quinn, J.L., et al. (2013).
890 Haplotype structure, adaptive history and associations with exploratory behaviour of the
891 DRD4 gene region in four great tit (*Parus major*) populations. Mol. Ecol. *22*, 2797–2809.

892 20. Nikhil, K.L., Abhilash, L., and Sharma, V.K. (2016). Molecular Correlates of Circadian
893 Clocks in Fruit Fly *Drosophila melanogaster* Populations Exhibiting early and late
894 Emergence Chronotypes. J. Biol. Rhythms *31*, 125–141.

895 21. Pegoraro, M., Flavell, L.M.M., Menegazzi, P., Colombi, P., Dao, P., Helfrich-Förster, C.,
896 and Tauber, E. (2020). The genetic basis of diurnal preference in *Drosophila*
897 melanogaster. BMC Genomics *21*, 596.

898 22. Burns, J.G., Svetec, N., Rowe, L., Mery, F., Dolan, M.J., Boyce, W.T., and Sokolowski,
899 M.B. (2012). Gene–environment interplay in *Drosophila melanogaster*: Chronic food
900 deprivation in early life affects adult exploratory and fitness traits. Proc. Natl. Acad. Sci.
901 *109*, 17239–17244.

902 23. Anreiter, I., Sokolowski, H.M., and Sokolowski, M.B. (2018). Gene–Environment
903 Interplay and Individual Differences in Behavior. Mind Brain Educ. *12*, 200–211.

904 24. Vogt, G. (2015). Stochastic developmental variation, an epigenetic source of phenotypic
905 diversity with far-reaching biological consequences. J. Biosci. *40*, 159–204.

906 25. Rey, S., Boltana, S., Vargas, R., Roher, N., and MacKenzie, S. (2013). Combining animal
907 personalities with transcriptomics resolves individual variation within a wild-type
908 zebrafish population and identifies underpinning molecular differences in brain function.
909 Mol. Ecol. *22*, 6100–6115.

910 26. Das, B., and de Bekker, C. (2022). Time-course RNASeq of *Camponotus floridanus*
911 forager and nurse ant brains indicate links between plasticity in the biological clock and
912 behavioral division of labor. BMC Genomics *23*, 57.

913 27. Pegoraro, M., Picot, E., Hansen, C.N., Kyriacou, C.P., Rosato, E., and Tauber, E. (2015).
914 Gene Expression Associated with Early and Late Chronotypes in *Drosophila*
915 melanogaster. Front. Neurol. *6*.

916 28. Sih, A., Mathot, K.J., Moirón, M., Montiglio, P.-O., Wolf, M., and Dingemanse, N.J.
917 (2015). Animal personality and state–behaviour feedbacks: a review and guide for
918 empiricists. Trends Ecol. Evol. *30*, 50–60.

919 29. Helm, B., Visser, M.E., Schwartz, W., Kronfeld-Schor, N., Gerkema, M., Piersma, T., and
920 Bloch, G. (2017). Two sides of a coin: ecological and chronobiological perspectives of
921 timing in the wild. Philos. Trans. R. Soc. B Biol. Sci. *372*, 20160246.

922 30. Krylov, V.V., Izvekov, E.I., Pavlova, V.V., Pankova, N.A., and Osipova, E.A. (2020).
923 Circadian rhythms in zebrafish (*Danio rerio*) behaviour and the sources of their
924 variability. Biol. Rev. *n/a*.

925 31. Mezan, S., Feuz, J.D., Deplancke, B., and Kadener, S. (2016). PDF Signaling Is an
926 Integral Part of the *Drosophila* Circadian Molecular Oscillator. Cell Rep. *17*, 708–719.

927 32. Menegazzi, P., Dalla Benetta, E., Beauchamp, M., Schlichting, M., Steffan-Dewenter, I.,
928 and Helfrich-Förster, C. (2017). Adaptation of Circadian Neuronal Network to
929 Photoperiod in High-Latitude European Drosophilids. Curr. Biol. *27*, 833–839.

930 33. Bertolini, E., Schubert, F.K., Zanini, D., Sehadová, H., and Helfrich-Förster, C. (2019).
931 Life at High Latitudes Does Not Require Circadian Behavioral Rhythmicity under
932 Constant Darkness. Curr. Biol. *29*, 3928–3936.

933 34. Beauchamp, M., Bertolini, E., Deppisch, P., Steubing, J., Menegazzi, P., and Helfrich-
934 Förster, C. (2018). Closely Related Fruit Fly Species Living at Different Latitudes
935 Diverge in Their Circadian Clock Anatomy and Rhythmic Behavior. J. Biol. Rhythms *33*,
936 602–613.

937 35. Deppisch, P., Prutscher, J.M., Pegoraro, M., Tauber, E., Wegener, C., and Helfrich-
938 Förster, C. (2022). Adaptation of *Drosophila melanogaster* to Long Photoperiods of
939 High-Latitude Summers Is Facilitated by the *ls-Timeless* Allele. J. Biol. Rhythms,
940 07487304221082448.

941 36. Lamaze, A., Chen, C., Leleux, S., Xu, M., George, R., and Stanewsky, R. (2022). A
942 natural timeless polymorphism allowing circadian clock synchronization in "white
943 nights." Nat. Commun. *13*, 1724.

944 37. Fischer, A., and Dorresteijn, A. (2004). The polychaete *Platynereis dumerilii* (Annelida):
945 a laboratory animal with spiralian cleavage, lifelong segment proliferation and a mixed
946 benthic/pelagic life cycle. BioEssays *26*, 314–325.

947 38. Bulla, M., Oudman, T., Bijleveld, A.I., Piersma, T., and Kyriacou, C.P. (2017). Marine
948 biorhythms: bridging chronobiology and ecology. Phil Trans R Soc B *372*, 20160253.

949 39. Veedin Rajan, V.B., Häfker, N.S., Arboleda, E., Poehn, B., Gossenreiter, T., Gerrard, E.,
950 Hofbauer, M., Mühlestein, C., Bileck, A., Gerner, C., et al. (2021). Seasonal variation in
951 UVA light drives hormonal and behavioural changes in a marine annelid via a ciliary
952 opsin. Nat. Ecol. Evol. *5*, 204–218.

953 40. Özpolat, B.D., Randel, N., Williams, E.A., Bezares-Calderón, L.A., Andreatta, G.,
954 Balavoine, G., Bertucci, P.Y., Ferrier, D.E.K., Gambi, M.C., Gazave, E., et al. (2021).
955 The Nereid on the rise: Platynereis as a model system. EvoDevo *12*, 10.

956 41. Ricevuto, E., Kroeker, K.J., Ferrigno, F., Micheli, F., and Gambi, M.C. (2014). Spatio-
957 temporal variability of polychaete colonization at volcanic CO_2 vents indicates high
958 tolerance to ocean acidification. Mar. Biol. *161*, 2909–2919.

959 42. Chouikh, N., Gillet, P., Langston, W.J., Cheggour, M., Maarouf, A., and Mouabad, A.
960 (2020). Spatial distribution and structure of benthic polychaete communities of Essaouira
961 intertidal rocky shores (Atlantic coast of Morocco). J. Oceanol. Limnol. *38*, 143–155.

962 43. Zantke, J., Ishikawa-Fujiwara, T., Arboleda, E., Lohs, C., Schipany, K., Hallay, N., Straw,
963 A.D., Todo, T., and Tessmar-Raible, K. (2013). Circadian and circalunar clock
964 interactions in a marine annelid. Cell Rep. *5*, 99–113.

965 44. Zurl, M., Poehn, B., Rieger, D., Krishnan, S., Rokvic, D., Veedin Rajan, V.B., Gerrard,
966 E., Schlichting, M., Orel, L., Ćorić, A., et al. (2022). Two light sensors decode moonlight
967 versus sunlight to adjust a plastic circadian/circalunidian clock to moon phase. Proc. Natl.
968 Acad. Sci. *119*, e2115725119.

969 45. Zantke, J., Bannister, S., Veedin-Rajan, V.B., Raible, F., and Tessmar-Raible, K. (2014).
970 Genetic and Genomic Tools for the Marine Annelid *Platynereis dumerilii*. Genetics *197*,
971 19–31.

972 46. Beer, K., and Helfrich-Förster, C. (2020). Model and Non-model Insects in
973 Chronobiology. Front. Behav. Neurosci. *14*, 601676.

974 47. Janssen, T., Husson, S.J., Lindemans, M., Mertens, I., Rademakers, S., Donck, K.V.,
975 Geysen, J., Jansen, G., and Schoofs, L. (2008). Functional Characterization of Three G

Protein-coupled Receptors for Pigment Dispersing Factors in *Caenorhabditis elegans*. J. Biol. Chem. *283*, 15241–15249.

48. Andreatta, G., Broyart, C., Borghgraef, C., Vadiwala, K., Kozin, V., Polo, A., Bileck, A., Beets, I., Schoofs, L., and Gerner, C. (2020). Corazonin signaling integrates energy homeostasis and lunar phase to regulate aspects of growth and sexual maturation in *Platynereis*. Proc. Natl. Acad. Sci. *117*, 1097–1106.

49. Bannister, S., Antonova, O., Polo, A., Lohs, C., Hallay, N., Valinciute, A., Raible, F., and Tessmar-Raible, K. (2014). TALENs Mediate Efficient and Heritable Mutation of Endogenous Genes in the Marine Annelid *Platynereis dumerilii*. Genetics *197*, 77–89.

50. Arboleda, E., Zurl, M., Waldherr, M., and Tessmar-Raible, K. (2019). Differential Impacts of the Head on *Platynereis dumerilii* Peripheral Circadian Rhythms. Front. Physiol. *10*, 900.

51. Thaben, P.F., and Westermark, P.O. (2014). Detecting Rhythms in Time Series with RAIN. J. Biol. Rhythms *29*, 391–400.

52. Zantke, J., Oberlerchner, H., and Tessmar-Raible, K. (2014). Circadian and Circalunar Clock Interactions and the Impact of Light in *Platynereis dumerilii*. In Annual, Lunar, and Tidal Clocks (Springer, Tokyo), pp. 143–162.

53. Liu, X., Liu, D., Shen, Y., Huang, M., Gao, L., Zhang, Z., Liu, B., Zhao, B., and Pang, Q. (2020). Matrix Metalloproteinases in Invertebrates. Protein Pept. Lett. *27*, 1068–1081.

54. Buckley, J.J., and Jessen, J.R. (2015). Matrix metalloproteinase function in non-mammalian model organisms. Front. Biosci. *7*, 168–183.

55. Small, C.D., and Crawford, B.D. (2016). Matrix metalloproteinases in neural development: a phylogenetically diverse perspective. Neural Regen. Res. *11*, 357–362.

56. Vaze, K.M., and Helfrich-Förster, C. (2021). The Neuropeptide PDF Is Crucial for Delaying the Phase of *Drosophila*'s Evening Neurons Under Long Zeitgeber Periods. J. Biol. Rhythms *36*, 442–460.

57. Menegazzi, P., Beer, K., Grebler, V., Schlichting, M., Schubert, F.K., and Helfrich-Förster, C. (2020). A Functional Clock Within the Main Morning and Evening Neurons of *D. melanogaster* Is Not Sufficient for Wild-Type Locomotor Activity Under Changing Day Length. Front. Physiol. *11*, 229.

58. Williams, J.A., and Sehgal, A. (2001). Molecular components of the circadian system in *Drosophila*. Annu. Rev. Physiol. *63*, 729–755.

59. Lin, Y., Stormo, G.D., and Taghert, P.H. (2004). The Neuropeptide Pigment-Dispersing Factor Coordinates Pacemaker Interactions in the *Drosophila* Circadian System. J. Neurosci. *24*, 7951–7957.

1011 60. Biro, P.A., and Stamps, J.A. (2010). Do consistent individual differences in metabolic rate
1012 promote consistent individual differences in behavior? Trends Ecol. Evol. *25*, 653–659.

1013 61. Claridge-Chang, A., Wijnen, H., Naef, F., Boothroyd, C., Rajewsky, N., and Young,
1014 M.W. (2001). Circadian Regulation of Gene Expression Systems in the *Drosophila* Head.
1015 Neuron *32*, 657–671.

1016 62. Miller, C.M., Page-McCaw, A., and Broihier, H.T. (2008). Matrix metalloproteinases
1017 promote motor axon fasciculation in the *Drosophila* embryo. Development *135*, 95–109.

1018 63. Anea, C.B., Ali, M.I., Osmond, J.M., Sullivan, J.C., Stepp, D.W., Merloiu, A.M., and
1019 Rudic, R.D. (2010). Matrix Metalloproteinase 2 and 9 Dysfunction Underlie Vascular
1020 Stiffness in Circadian Clock Mutant Mice. Arterioscler. Thromb. Vasc. Biol. *30*, 2535–
1021 2543.

1022 64. Halter, K. (2020). The role of extracellular proteases, matrix metalloproteinase-2 and -9,
1023 in regulating the mammalian circadian clock. PhD thesis, University of Tennessee, USA.

1024 65. Sivachenko, A., Li, Y., Abruzzi, K.C., and Rosbash, M. (2013). The Transcription Factor
1025 Mef2 Links the *Drosophila* Core Clock to *Fas2*, Neuronal Morphology, and Circadian
1026 Behavior. Neuron *79*, 281–292.

1027 66. Pivarciova, L., Vaneckova, H., Provaznik, J., Wu, B.C., Pivarci, M., Peckova, O.,
1028 Bazalova, O., Cada, S., Kment, P., Kotwica-Rolinska, J., et al. (2016). Unexpected
1029 Geographic Variability of the Free Running Period in the Linden Bug *Pyrrhocoris*
1030 *apterus*. J. Biol. Rhythms, 0748730416671213.

1031 67. Svanbäck, R., and Bolnick, D.I. (2007). Intraspecific competition drives increased
1032 resource use diversity within a natural population. Proc. R. Soc. B Biol. Sci. *274*, 839–
1033 844.

1034 68. Lloyd, E., Chhouk, B., Conith, A.J., Keene, A.C., and Albertson, R.C. (2021). Diversity
1035 in rest–activity patterns among Lake Malawi cichlid fishes suggests a novel axis of habitat
1036 partitioning. J. Exp. Biol. *224*.

1037 69. Mittelbach, G.G., Ballew, N.G., and Kjelvik, M.K. (2014). Fish behavioral types and their
1038 ecological consequences. Can. J. Fish. Aquat. Sci. *71*, 927–944.

1039 70. Morozov, A., Pasternak, A.F., and Arashkevich, E.G. (2013). Revisiting the Role of
1040 Individual Variability in Population Persistence and Stability. PLOS ONE *8*, e70576.

1041 71. Häfker, N.S., Connan-McGinty, S., Hobbs, L., McKee, D., Cohen, J.H., and Last, K.S.
1042 (2022). Animal behavior is central in shaping the realized diel light niche. Commun. Biol.
1043 *5*, 562.

1044 72. Miller, C.T., Gire, D., Hoke, K., Huk, A.C., Kelley, D., Leopold, D.A., Smear, M.C.,
1045 Theunissen, F., Yartsev, M., and Niell, C.M. (2022). Natural behavior is the language of
1046 the brain. Curr. Biol. *32*, R482–R493.

1047 73. Keplinger, S. (2010). Influence of the adult eyes on circadian and lunar rhythms in
1048 *Platynereis dumerilii*. Diploma thesis, University of Vienna, Austria.

1049 74. Hammer, S. (2012). Target tissues of melatonin and PDF in *Platynereis*. Diploma thesis,
1050 University of Vienna, Austria.

1051 75. R Development Core Team (2013). R: A language and environment for statistical
1052 computing. https://www.r-project.org.

1053 76. Love, M.I., Huber, W., and Anders, S. (2014). Moderated estimation of fold change and
1054 dispersion for RNA-seq data with DESeq2. Genome Biol. *15*, 550.

1055 77. Alexa, A., and Rahnenführer, J. (2009). Gene set enrichment analysis with topGO. R
1056 package version 2.46.0. https://bioconductor.org/packages/topGO/.

1057 78. Warnes, G.R., Bolker, B., Bonebakker, L., Gentleman, R., Liaw, W.H.A., Lumley, T.,
1058 Maechler, M., Magnusson, A., Moeller, S., Schwartz, M., et al. (2016). gplots: Various R
1059 Programming Tools for Plotting Data. version 3.1.1. https://CRAN.R-
1060 project.org/package=gplots.

1061 79. Neuwirth, E. (2014). RColorBrewer: ColorBrewer Palettes R package version 1.1-2.
1062 https://CRAN.R-project.org/package=RColorBrewer.

1063 80. Schindelin, J., Arganda-Carreras, I., Frise, E., Kaynig, V., Longair, M., Pietzsch, T.,
1064 Preibisch, S., Rueden, C., Saalfeld, S., Schmid, B., et al. (2012). Fiji: an open-source
1065 platform for biological-image analysis. Nat. Methods *9*, 676–682.

1066 81. Schmid, B., Helfrich-Förster, C., and Yoshii, T. (2011). A New ImageJ Plug-in
1067 "ActogramJ" for Chronobiological Analyses. J. Biol. Rhythms *26*, 464–467.

1068 82. Patro, R., Duggal, G., Love, M.I., Irizarry, R.A., and Kingsford, C. (2017). Salmon
1069 provides fast and bias-aware quantification of transcript expression. Nat. Methods *14*,
1070 417–419.

1071 83. Li, H., Handsaker, B., Wysoker, A., Fennell, T., Ruan, J., Homer, N., Marth, G.,
1072 Abecasis, G., Durbin, R., and 1000 Genome Project Data Processing Subgroup (2009).
1073 The Sequence Alignment/Map format and SAMtools. Bioinformatics *25*, 2078–2079.

1074 84. Martin, M. (2011). Cutadapt removes adapter sequences from high-throughput
1075 sequencing reads. EMBnet.journal *17*, 10–12.

1076 85. Andrews, S. (2010). FastQC: a quality control tool for high throughput sequence data.
1077 Babraham Institute, Cambridge, UK.
1078 http://www.bioinformatics.babraham.ac.uk/projects/fastqc/.

1079 86. Mistry, J., Chuguransky, S., Williams, L., Qureshi, M., Salazar, G.A., Sonnhammer,
1080 E.L.L., Tosatto, S.C.E., Paladin, L., Raj, S., Richardson, L.J., et al. (2021). Pfam: The
1081 protein families database in 2021. Nucleic Acids Res. *49*, D412–D419.

1082 87. Hauenschild, C. (1954). Über das lunarperiodische Schwärmen von *Platynereis Dumerilii*
1083 in Laboratoriumszuchten. Naturwissenschaften *41*, 556–557.

1084 88. Ranzi, S. (1931). Maturita sessuale degli Anellidi e fasi lunari. Boll Soc Ital Biol Sper *6*,
1085 18.

1086 89. Ayers, T., Tsukamoto, H., Gühmann, M., Veedin-Rajan, V.B., and Tessmar-Raible, K.
1087 (2018). A G_o-type opsin mediates the shadow reflex in the annelid *Platynereis dumerilii*.
1088 BMC Biol. *16*, 41.

1089 90. Madeira, F., Park, Y.M., Lee, J., Buso, N., Gur, T., Madhusoodanan, N., Basutkar, P.,
1090 Tivey, A.R.N., Potter, S.C., Finn, R.D., et al. (2019). The EMBL-EBI search and
1091 sequence analysis tools APIs in 2019. Nucleic Acids Res. *47*, W636–W641.

1092 91. Trifinopoulos, J., Nguyen, L.-T., von Haeseler, A., and Minh, B.Q. (2016). W-IQ-TREE:
1093 a fast online phylogenetic tool for maximum likelihood analysis. Nucleic Acids Res. *44*,
1094 W232–W235.

1095 92. Truett, G. e., Heeger, P., Mynatt, R. l., Truett, A. a., Walker, J. a., and Warman, M. l.
1096 (2000). Preparation of PCR-Quality Mouse Genomic DNA with Hot Sodium Hydroxide
1097 and Tris (HotSHOT). BioTechniques *29*, 52–54.

1098 93. Steinkellner, E. (2012). Regulation and function of conserved *Platynereis* hormones.
1099 Diploma thesis, University of Vienna, Austria.

1100 94. Schenk, S., Bannister, S.C., Sedlazeck, F.J., Anrather, D., Minh, B.Q., Bileck, A., Hartl,
1101 M., von Haeseler, A., Gerner, C., Raible, F., et al. (2019). Combined transcriptome and
1102 proteome profiling reveals specific molecular brain signatures for sex, maturation and
1103 circalunar clock phase. eLife *8*, e41556.

1104 95. Livak, K.J., and Schmittgen, T.D. (2001). Analysis of relative gene expression data using
1105 real-time quantitative PCR and the $2^{-\Delta\Delta CT}$ method. Methods *25*, 402–408.

1106 96. Manni, M., Berkeley, M.R., Seppey, M., Simão, F.A., and Zdobnov, E.M. (2021).
1107 BUSCO Update: Novel and Streamlined Workflows along with Broader and Deeper
1108 Phylogenetic Coverage for Scoring of Eukaryotic, Prokaryotic, and Viral Genomes. Mol.
1109 Biol. Evol. *38*, 4647–4654.

1110 97. Benjamini, Y., and Hochberg, Y. (1995). Controlling the False Discovery Rate: A
1111 Practical and Powerful Approach to Multiple Testing. J. R. Stat. Soc. Ser. B Methodol.
1112 *57*, 289–300.

1113 98. Bryant, D.M., Johnson, K., DiTommaso, T., Tickle, T., Couger, M.B., Payzin-Dogru, D.,
1114 Lee, T.J., Leigh, N.D., Kuo, T.-H., Davis, F.G., et al. (2017). A Tissue-Mapped Axolotl
1115 De Novo Transcriptome Enables Identification of Limb Regeneration Factors. Cell Rep.
1116 *18*, 762–776.

1117 99. Altschul, S.F., Gish, W., Miller, W., Myers, E.W., and Lipman, D.J. (1990). Basic local
1118 alignment search tool. J. Mol. Biol. *215*, 403–410.

1119 100. Suzek, B.E., Wang, Y., Huang, H., McGarvey, P.B., Wu, C.H., and the UniProt
1120 Consortium (2015). UniRef clusters: a comprehensive and scalable alternative for
1121 improving sequence similarity searches. Bioinformatics *31*, 926–932.

1122 101. Alexa, A., Rahnenführer, J., and Lengauer, T. (2006). Improved scoring of functional
1123 groups from gene expression data by decorrelating GO graph structure. Bioinformatics
1124 *22*, 1600–1607.